DALTON
FULL PAPER

Donor–acceptor complexes incorporating ferrocenes: spectroelectrochemical characterisation, quadratic hyperpolarisabilities and the effects of oxidising and reducing agents

Michael Malaun,[a] Ralph Kowallick,[a] Andrew M. McDonagh,[a] Massimo Marcaccio,[a] Rowena L. Paul,[a] Inge Asselberghs,[b] Koen Clays,[b] André Persoons,[b] Benno Bildstein,[c] Céline Fiorini,[d] Jean-Michel Nunzi,†[d] Michael D. Ward *[a] and Jon A. McCleverty *[a]

[a] *School of Chemistry, University of Bristol, Cantock's Close, Bristol, UK BS8 1TS. E-mail: jon.mccleverty@bristol.ac.uk; mike.ward@bristol.ac.uk*
[b] *Laboratory of Chemical and Biological Dynamics, Centre for Research on Molecular Electronics and Photonics, University of Leuven, Celestijnenlaan 200D, B-300, Leuven, Belgium*
[c] *Institute for General, Inorganic and Theoretical Chemistry, University of Innsbruck, Innrain 52A, 6020 Innsbruck, Austria*
[d] *LETI (CEA-Technologies Avancés), DEIN/SPE Group Composants Organiques, CEA Saclay, F-91191 Gif-sur-Yvette cedex, France*

Received 31st May 2001, Accepted 7th August 2001
First published as an Advance Article on the web 1st October 2001

The donor–acceptor complexes $[Fe(C_5H_5)\{C_5H_4QNHM(NO)(Tp^{Me,Me})X\}]$ {$Tp^{Me,Me}$ = tris(3,5-dimethylpyrazolyl)-borate; Q = nothing, M = Mo, X = Cl, Br, I; M = W, X = Cl; Q = C_6H_4, M = Mo, X = Cl, Br, I; M = W, X = Cl; Q = CH=CHC_6H_4 or N=NC_6H_4, M = Mo, X = Cl), which contain 16-valence electron metal nitrosyl centres, $[Fe(C_5H_5)\{C_5H_4QpyMo(NO)(Tp^{Me,Me})Cl\}]$ (py = 4-pyridyl; Q = CH=CH, CH=CHCO, N=CH and C_6H_4CH=CH), $[Fe(C_5Me_4H)\{C_5H_4CH=CHpyMo(NO)(Tp^{Me,Me})Cl\}]$ and $[Fe(C_5Me_4H)(C_5Me_4QpyZ)]$ {Q = CH=CH or CH=N, Z = Mo(NO)$(Tp^{Me,Me})$Cl or $W(CO)_5$; Q=2,4-CH=CH(C_4H_2S)CH=CH, Z = $W(CO)_5$ or Me^+I^-}, some of which contain 17-valence electron molybdenum nitrosyl centres, and $[Fe(C_5Me_4H)\{C_5Me_4CH=CH(C_4H_2S)CH=CHpy\}]$, have been characterised electrochemically, by their electronic spectra, and spectroelectrochemically. Hyper-Rayleigh scattering was used to determine the first hyperpolarisability, β, the data showing that (a) β is dependent on the metal in the acceptor fragment, (b) β increased when Cl or Br was replaced by I and (c) β increased when the number of methyl groups on the cyclopentadienyl rings increased. The β-values for comparable complexes containing {Mo(NO)$(Tp^{Me,Me})$Cl} and $\{W(CO)_5\}$ moieties were similar. Chemical oxidation of the ferrocenyl or chemical reduction of the molybdenum nitrosyl acceptor fragments in selected complexes caused a reduction of between 25% and 100% in the NLO response. X-Ray structural studies of $[Fe(C_5H_5)\{C_5H_4NHMo(NO)(Tp^{Me,Me})Cl\}]$ ($P\bar{1}$) and $[Fe(C_5Me_4H)\{C_5Me_4CH=CHpyMo(NO)(Tp^{Me,Me})Cl\}]$ ($P\bar{1}$) are reported.

Introduction

Because of potential applications in optoelectronics technology, there has been sustained interest in the syntheses and development of molecular materials with second-order non-linear optical (NLO) properties. Most effort has focused on organic molecules because of their promise of large NLO responses, fast response times, the considerable ease of synthetic modification which can optimise optoelectronic behaviour, and their potential for facile processability.[1] Metal–organic compounds also have considerable NLO potential[2] and although applications remain more of a dream than a reality, the addition of a metal to an otherwise organic material can have significant "added value" resulting from particular manipulable redox, magnetic and structural properties.[3]

From a wealth of experimental and theoretical studies, it is clear that for a molecule to have significant NLO potential, it should have excited states close in energy to the ground state, the electronic transitions from the ground to the excited states should have a high oscillator strength (*i.e.* the absorptions must be strong), and there must be a large difference between the dipole moments of the ground and excited states.[4] These requirements are normally satisfied in molecules containing donor and acceptor moieties connected by conjugated π-systems and should lead to large values of the first molecular hyperpolarisability, β. In the solid state, large values of β may be reflected in significant values of $\chi^{(2)}$, the second order susceptibility, provided that the molecule crystallises in a polar non-centrosymmetric space group. Many organometallic compounds which fulfil these broad criteria contain ferrocenyl derivatives as electron-donors and metal carbonyl or nitrosyl fragments as electron-acceptors.[5]

Our interest in this area arose from our own deductions that metal complexes based on molybdenum and tungsten nitrosyl moieties, stabilised by tris(3,5-dimethylpyrazolyl)borate ($Tp^{Me,Me}$) and attached to phenolato or anilido groups, were strongly polarising and might therefore be able to act as electron-acceptor termini of dipolar complexes having second-order NLO properties.[6] A particular advantage of the {M(NO)-$(Tp^{Me,Me})$XY} fragment is that most of the components can be relatively easily varied: for example, M = Mo or W; X = Cl, Br, I;

† Current address: Laboratoire POMA, UMR-CNRS 6136, Université d'Angers, F49045, Angers cedex, France.

DOI: 10.1039/b104791b

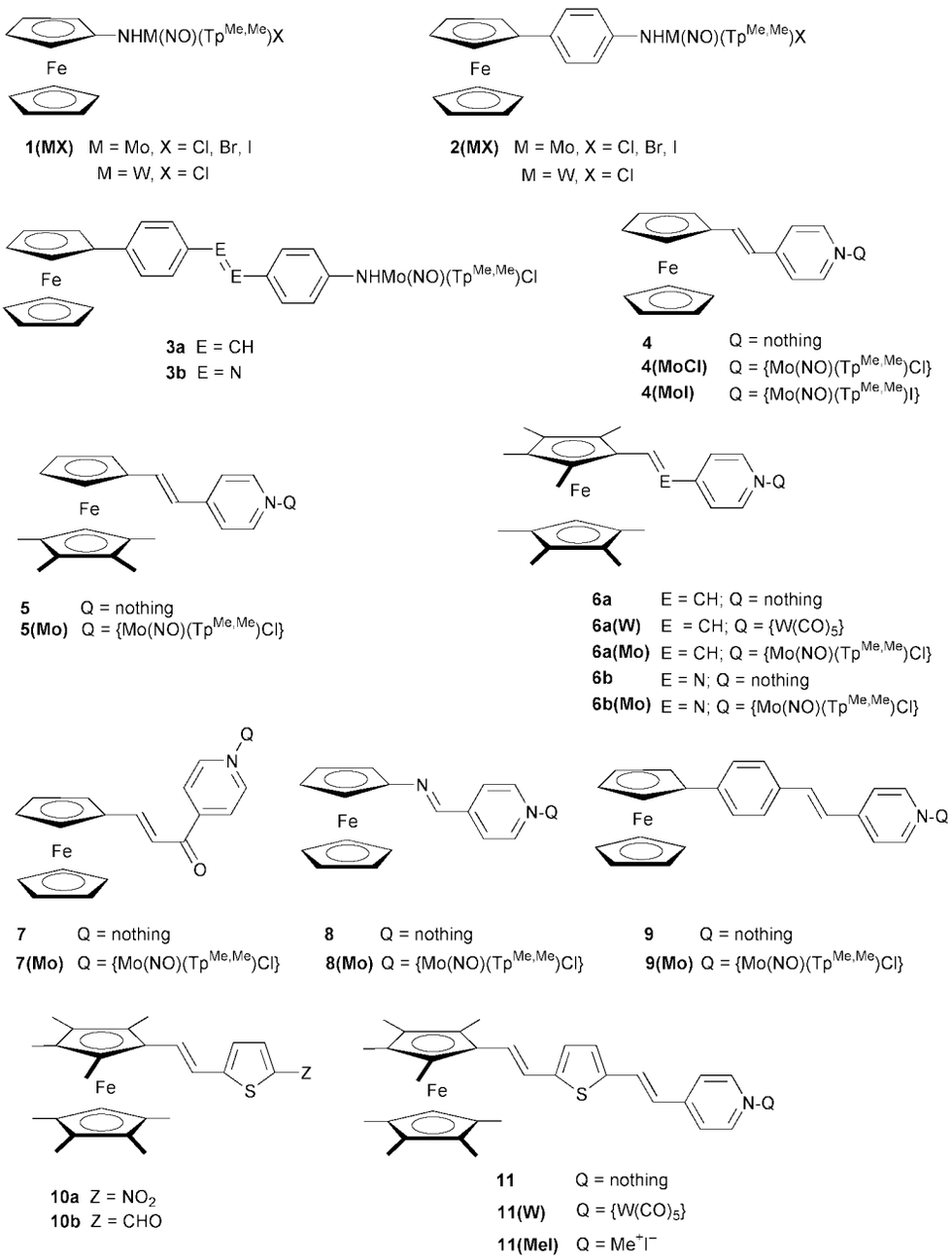

Scheme 1 The dipolar organometallic complexes discussed in this paper.

and Y (the ligand which connects to the electron-donor fragment) can be phenolate, anilide, or pyridyl. There is therefore substantial scope for investigating the effect of varying M, X and Y on the NLO response of dipolar species containing {M(NO)(Tp^{Me,Me})XY}.

Our earlier work based on Kurtz powder tests showed that the complexes [FcC_6H_3(R)E=EC_6H_3(R)NH{M(NO)(Tp^{Me,Me})X}] {Fc = ferrocenyl; R = H or 3-Me, E = N or CH, M = Mo or W, X = Cl, Br or I (substituted derivatives of series **3**, Scheme 1)} did indeed exhibit second harmonic generation (SHG), *i.e.* frequency doubling.[7] Crystallographic studies of several NLO-active complexes showed not only that they crystallised in a polar non-centrosymmetric space group ($P2_1$) but also that the molecules in the unit cells were favourably oriented to produce phase matching.[8] However, substituting either the ferrocenyl or the metal nitrosyl fragment by, respectively, a more conventional donor (*e.g.* NMe_2) or acceptor (*e.g.* NO_2) group caused loss of the frequency doubling behaviour in the solid state. It therefore seemed possible that the combination of the near-cylindrical ferrocenyl and the near-spherical {M(NO)(Tp^{Me,Me})X} (X = halide) groups was essential to the crystal packing which facilitated the SHG behaviour of these compounds.

While these *solid state* Kurtz test data were encouraging, hinting that there might be electronic effects derived from metal and ligand substituents as well as structural effects influencing the NLO response,[6] they did not provide *quantitative* information. Consequently, we have undertaken an investigation of the SHG capabilities of these compounds *in solution* in order to determine what effect metal and substituent variations have on their molecular second-order optical nonlinearities.

This paper reports the preparation of new complexes of the type Fc–L–{M(NO)(Tp^{Me,Me})X}, (where Fc is a ferrocenyl derivative including tetramethyl- and octamethyl-ferrocene derivatives, L is a conjugated linking group, and M = Mo, W), together with two X-ray structural studies, electrochemical and spectroelectrochemical results, and quadratic NLO data for an extensive series of complexes of this general class. In addition, we have exploited the redox activity of these complexes to examine the NLO response of selected complexes in different oxidation states. Redox-switching of NLO behaviour is an area that has received very little attention, despite the large number

of ferrocenyl-based donor–acceptor molecules which would be amenable to such treatment.

Experimental

General details

The starting materials $[M(NO)(Tp^{Me,Me})X_2]$ (M = Mo or W; X = Cl, Br, I),[9,10] ferrocenylamine,[11] 4-aminophenylferrocene,[12] $[Fe(C_5H_5)(C_5H_4CH{=}CHC_5H_4N)]$ (**4**),[13] pentamethylferrocenealdehyde,[14] {(1′,2,2′,3,3′,4,4′,5-octamethylferrocenyl)methyl}triphenylphosphonium bromide,[15] octamethylferrocene,[16] and $[Fe(C_5Me_4H)\{C_5Me_4CH{=}CH(C_4H_4S)CHO\}]$ (**10b**)[17] were prepared as previously described. Solvents for reactions and electrochemistry were pre-dried, and all reactions were carried out under dinitrogen.

The following instruments were used for routine spectroscopic work: ^{1}H NMR spectroscopy, JEOL GX-270 or λ-300 spectrometers (in $CDCl_3$ unless otherwise stated); electron-impact and fast-atom bombardment (FAB) mass spectrometry, a VG-Autospec; EPR spectrometry, a Bruker ESP-300E; UV-VIS spectrophotometry, a Perkin-Elmer Lambda 2; FT-IR spectrometry, a Perkin-Elmer 1600 instrument (in CH_2Cl_2 solution). UV/VIS/NIR spectroelectrochemistry was carried out using a home-built OTTLE cell mounted in the sample compartment of a Perkin-Elmer Lambda 19 spectrometer, according to a procedure described previously.[18]

Electrochemical measurements (cyclic and/or square wave voltammetry) were carried out using a PC-controlled EC&G PAR model 273A potentiostat, with platinum wire working and counter electrodes, a saturated calomel reference electrode or silver wire pseudo-reference electrode, dry CH_2Cl_2 as solvent and $[NBu^n_4][PF_6]$ (*ca.* 0.1 mol dm^{-3}) as base electrolyte. Metal complexes for electrochemical examination were *ca.* 10^{-3} M. Ferrocene was added as internal standard, and all potentials are quoted relative to the ferrocenium/ferrocene couple.

Hyper-Rayleigh scattering measurements were performed as follows. An injection-seeded Nd:YAG laser (Q-switched Nd:YAG Quanta Ray GCR5, 1064 nm, 8 ns pulses, 10 Hz) was focused into a cyclindrical cell (7 cm^3) containing the sample, which was a *ca.* 4×10^{-5} M solution of the complex in CH_2Cl_2. The intensity of the incident beam was varied by rotation of a half-wave plate placed between crossed polarizers. Part of the laser pulse was sampled by a photodiode to measure the vertically polarised incident light intensity. The frequency-doubled light was collected by an efficient condenser system and was detected by a photomultiplier. The harmonic scattering and linear scattering were distinguished by appropriate filters; gated integrators were used to obtain intensities of the incident and scattered light. The absence of luminescence contribution to the harmonic signal was confirmed by using interference filters of different wavelengths near 532 nm. All measurements were referenced to *p*-nitroaniline.[19] Solutions were sufficiently dilute that absorption of scattered second-harmonic light was negligible. Further details of the experimental procedure have been described elsewhere.[20] Data for the oxidised species were obtained by dissolving the separately-prepared salts (*vide infra*) in dichloromethane, solutions being typically 10^{-5}–10^{-6} M, or by oxidising the complexes with $[Bu^n_4N][Br_3]$, as previously described.[21]

The time-resolved non-degenerate six-wave mixing (6WM) experiments were carried out in argon-degassed dimethylformamide (dmf) solutions using a picosecond Nd:YAG laser operating at 1064 nm. The technique is a purely optical one which permits characterisation of the β tensor values and resonance characteristics in solution. Details of the experimental procedures have been described elsewhere.[22] Two compounds were measured, **2**(**MoCl**) and **3b**, each compound being typically *ca.* 10^{-4} M in dmf. Their UV/VIS/NIR spectra were measured before reduction and the six-wave mixing experiment was carried out in order to determine the intensity of the second harmonic response $I_{2\omega}^{6WM}$. Cobaltocene in slight excess was then added, the mixture shaken to ensure that everything had dissolved, and the procedure with the electronic spectral and six-wave mixing measurements repeated. This permitted measurement of the second harmonic response and evaluation of β^{6WM} by comparison to the etalon dye Disperse-Red 1 ([4-{*N*-(2-hydroxyethyl)-*N*-ethyl}-amino-4′-nitroazobenzene], DR1).[22]

Syntheses

$[Fe(C_5H_5)\{C_5H_4NHMo(NO)(Tp^{Me,Me})Cl\}]$, 1(MoCl). A mixture of ferrocenylamine (0.20 g), $[Mo(NO)(Tp^{Me,Me})Cl_2]$ (0.25 g) and NEt_3 (0.7 cm^3) was heated and stirred in toluene (20 cm^3, 95 °C) for 4 h. The dark green solution was cooled and evaporated to dryness *in vacuo*, and the components of the residue purified by column chromatography on silica using CH_2Cl_2. The major green band was collected and evaporated to dryness to yield the compound as green microcrystals (0.17 g, 53%). Found: C, 45.3; H, 5.2; N, 16.7. $C_{25}H_{32}N_8BClOFeMo$ requires C, 45.6; H 4.9; N, 17.0%. FABMS: *m*/*z* 660 [M$^+$]; IR 1640 (ν_{NO}), 2546 (ν_{BH}), 3222 (ν_{NH}) cm^{-1}; ^{1}H NMR (CD_2Cl_2): δ 12.19 (1H, s, NH); 5.96, 5.88, 5.76 {each signal 1H, s, $(Me_2C_3N_2H)_3$}; 5.65, 4.78, 4.41,4.08 (each signal 1H, m, C_5H_4); 4.51 (5H, s, C_5H_5); 2.68, 2.60, 2.42, 2.36, 2.31, 1.98 {each signal 3H, s, $(Me_2C_3N_2H)_3$}.

$[Fe(C_5H_5)\{C_5H_4NHMo(NO)(Tp^{Me,Me})Br\}]$, 1(MoBr). A mixture of ferrocenylamine (0.08 g), $[Mo(NO)(Tp^{Me,Me})Br_2]$ (0.12 g) and NEt_3 (0.3 cm^3) was heated and stirred in toluene (10 cm^3, 100 °C) for 2 h. The mixture was cooled and evaporated to dryness *in vacuo*, the components of the residue being purified by column chromatography on silica using CH_2Cl_2 containing hexane (20%). The major green band was collected, evaporated to dryness and the solid recrystallised from CH_2Cl_2/hexane yielding the compound as green microcrystals (0.06 g, 43%). Found: C, 42.9; H, 5.0; N, 16.0. $C_{25}H_{32}N_8BBrOFeMo$ requires C, 42.7; H 4.6; N, 15.9%. FABMS: *m*/*z* 704 [M$^+$]; IR 1643 (ν_{NO}), 2536 (ν_{BH}), 3215 (ν_{NH}) cm^{-1}; ^{1}H NMR (CD_2Cl_2): δ 12.31 (1H, s, NH); 5.90, 5.80, 5.66 {each signal 1H, s, $(Me_2C_3N_2H)_3$}; 5.58, 4.75, 4.35, 4.02 (each signal 1H, m, C_5H_4); 4.45 (5H, s, C_5H_5); 2.66, 2.54, 2.35, 2.28, 2.23, 1.87 {3H, s, $(Me_2C_3N_2H)_3$}.

$[Fe(C_5H_5)\{C_5H_4NHMo(NO)(Tp^{Me,Me})I\}]$, 1(MoI). This was prepared in the same way as **1**(**MoBr**) above, using ferrocenylamine (0.15 g), $[Mo(NO)(Tp^{Me,Me})I_2]$ (0.25 g) and NEt_3 (0.5 cm^3) in toluene (15 cm^3, 100 °C). The mixture was cooled and evaporated to dryness under reduced pressure. The compound was obtained as green microcrystals (0.13 g, 47%). Found: C, 40.4; H, 4.0; N, 15.5. $C_{25}H_{32}N_8BIOFeMo$ requires C, 40.0; H 4.3; N, 14.9%. FABMS: *m*/*z* 752 [M$^+$]; IR 1643 (ν_{NO}), 2547 (ν_{BH}), 3213 (ν_{NH}) cm^{-1}; ^{1}H NMR (CD_2Cl_2): δ 12.59 (1H, s, NH); 6.00, 5.87, 5.73 {each signal 1H, s, $(Me_2C_3N_2H)_3$}; 5.67, 4.87, 4.45, 4.13 (each signal 1H, m, C_5H_4); 4.54 (5H, s, C_5H_5) 2.79, 2.63, 2.46, 2.36, 2.31, 1.91 {each signal 3H, s, $(Me_2C_3N_2H)_3$}.

$[Fe(C_5H_5)\{C_5H_4NHW(NO)(Tp^{Me,Me})Cl\}]$, 1(WCl). A mixture of ferrocenylamine (0.15 g), $[W(NO)(Tp^{Me,Me})Cl_2]$ (0.22 g) and NEt_3 (0.8 cm^3) was heated and stirred in toluene (25 cm^3, 100 °C) for 4 h. The mixture was cooled and evaporated to dryness *in vacuo*, the components of the residue being purified by column chromatography on silica using CH_2Cl_2 containing hexane (30%). The compound was purified by column chromatography on silica using CH_2Cl_2/hexane and afterwards recrystallised from CH_2Cl_2/hexane to yield the compound as blue microcrystals (0.07 g, 26%). Found (as $0.3CH_2Cl_2$ solvate): C, 39.5; H, 3.8; N, 14.5. $C_{25}H_{32}N_8BClOFeW$ requires C, 39.4; H 4.3; N, 14.5%. FABMS: *m*/*z* 746 [M$^+$]; IR 1607 and 1620 (ν_{NO}), 2547 (ν_{BH}), 3295 (ν_{NH}) cm^{-1}; ^{1}H NMR (CD_2Cl_2): δ 10.48 (1H, s,

NH); 6.01, 5.90, 5.79 {1H, s, $(Me_2C_3N_2H)_3$}; 5.52, 4.43, 4.10, 3.94 (each signal 1H, m, C_5H_4); 4.39 (5H, s, C_5H_5); 2.73, 2.64, 2.42, 2.35, 2.31, 2.09 {each signal 3H, s, $(Me_2C_3N_2H)_3$}.

[Fe(C_5H_5){$C_5H_4C_6H_4NHMo(NO)(Tp^{Me,Me})Br$}], 2(MoBr). A mixture of 4-ferrocenylaniline (0.12 g), $[Mo(NO)(Tp^{Me,Me})Br_2]$ (0.20 g) and NEt_3 (0.3 cm^3) was stirred and refluxed in toluene (13 cm^3) for 5 h. The mixture was cooled and evaporated to dryness *in vacuo*, the components of the residue being purified by column chromatography on silica using CH_2Cl_2 containing hexane (30%). The compound was recrystallised from CH_2Cl_2/hexane to give black microcrystals (0.12 g, 45%). Found: C, 47.6; H, 4.9; N, 14.1. $C_{31}H_{36}N_8BClOFeMo$ requires C, 47.8; H 4.7; N, 14.4%. FABMS: *m*/*z* 780 [M^+]; IR 1651 (ν_{NO}), 2550 (ν_{BH}), 3264 (ν_{NH}) cm^{-1}; ^{1}H NMR (CD_2Cl_2): δ 12.92 (1H, s, NH); 7.53, 7.45 {2H, d, J = 8.6; 2H, d, J = 8.7, C_6H_4}; 5.96, 5.93, 5.83 {each signal 1H, s, $(Me_2C_3N_2H)_3$} 4.72, 4.40 (each signal 2H, m, C_5H_4); 4.07 (5H, s, C_5H_5); 2.67, 2.46, 2.43, 2.40, 2.39, 2.01 {each signal 3H, s, $(Me_2C_3N_2H)_3$}.

[Fe(C_5H_5){$C_5H_4CH{=}CHC_5H_4NMo(NO)(Tp^{Me,Me})I$}], 4(MoI). A mixture of $[Mo(NO)(Tp^{Me,Me})I_2]$ (0.20 g), compound **4** (0.08 g) and NEt_3 (0.3 cm^3) in toluene (28 cm^3) was refluxed for 3 h, allowed to cool and evaporated to dryness *in vacuo*. The crude product was purified by column chromatography on silica using, initially, CH_2Cl_2/hexane (9 : 1 v/v) to remove traces of impurities and then CH_2Cl_2 containing THF (1%) to elute the product. The compound was obtained after recrystallization from CH_2Cl_2/hexane as purple crystals (0.09 g, 40%). Found (as $1.2CH_2Cl_2$ solvate): C, 42.2; H, 4.4; N, 11.9. $C_{32}H_{37}N_8$-BIOFeMo requires C, 42.4; H 4.2; N, 11.9%. FABMS: *m*/*z* 841 [M^+]; IR 1597 (ν_{NO}), 2539 (ν_{BH}) cm^{-1}; EPR: g_{iso} 2.006 (A_{Mo} 45.2 G).

[Fe(C_5Me_5)($C_5H_4CH{=}CHC_5H_4N$)], 5. A solution of lithium diisopropylamide (2.56 mmol) in THF (15 cm^3), prepared *in situ* before use from equimolar amounts of n-butyllithium and diisopropylamine at −3 °C under N_2, was added dropwise to 4-methylpyridine in THF (10 cm^3), the mixture being stirred for 50 min at −3 °C. Pentamethylferrocene aldehyde (0.66 g, 2.33 mmol) dissolved in THF (10 cm^3) was then added dropwise to the solution and the mixture was stirred overnight at RT. The mixture was then quenched with water (10 cm^3), concentrated *in vacuo*, and extracted with several portions of CH_2Cl_2. The extracts were combined, dried over $MgSO_4$, filtered and evaporated to dryness *in vacuo* affording the intermediate alcohol which was used for dehydration without any further purification. It was dissolved in dry pyridine (9 cm^3) and a solution of $POCl_3$ (0.30 cm^3, 3.22 mmol) in dry pyridine (5 cm^3) was added dropwise under N_2. After stirring for 3 h at room temperature unde N_2 the mixture was quenched with ice and evaporated to dryness. The crude compound was dissolved in water (30 cm^3) and the solution was made slightly basic with NaOH. The product was extracted with several portions of CH_2Cl_2, the solution was dried over $MgSO_4$, filtered and evaporated to dryness. The residue was dissolved in the minimum volume of CH_2Cl_2 and was chromatographed on alumina (Brockmann activity V) using CH_2Cl_2/hexane (1 : 1 v/v) as eluant. After evaporation of the red layer, the desired compound was isolated as a red powder (0.53 g, 63%). Found: C, 73.3; H, 6.9; N, 3.6. $C_{22}H_{25}FeN$ requires C, 73.5; H, 7.0; N, 3.9%. EIMS: *m*/*z* 359 [M^+]; ^{1}H NMR (CD_2Cl_2): δ 8.47, 7.28 (2H, m, $C_5H_4N^{2,6}$; 2H, m, $C_5H_4N^{3,5}$); 6.95, 6.48 (1H, d, J = 16.1; 1H, d, J = 16.1, HCCH); 3.95, 3.92 (2H, t, J = 1.8; 2H, t, J = 1.8, C_5H_4); 1.81 (15H, s, CH_3).

[Fe(C_5Me_5){$C_5H_4CH{=}CHC_5H_4NMo(NO)(Tp^{Me,Me})Cl$}], 5(Mo). A mixture of **5** (0.11 g), $[Mo(NO)Tp^{Me,Me}Cl_2]$ (0.16 g) and NEt_3 (1 cm^3) was stirred and refluxed in toluene (50 cm^3) for 15 h. The mixture was cooled, evaporated *in vacuo* and the residue dissolved in the minimum volume of CH_2Cl_2 and chromatographed on silica. Initial elution with CH_2Cl_2/hexane (9 : 1 v/v) eluted traces of unreacted $[Mo(NO)(Tp^{Me,Me})Cl_2]$ and $[\{Mo(NO)(Tp^{Me,Me})Cl\}_2O]$. Changing the solvent to CH_2Cl_2 containing THF (1%) allowed elution of the product which was recrystallised from CH_2Cl_2/hexane giving the desired compound as purple microcrystals (0.11 g, 46%). Found: C, 53.0; H, 5.6; N, 13.2. $C_{37}H_{47}N_7ClBOFeMo$ (as $0.25CH_2Cl_2$ solvate) requires C, 53.3; H, 5.7; N, 13.4%. FABMS: *m*/*z* 819 [M^+]; IR 1600 (ν_{NO}), 2543 (ν_{BH}) cm^{-1}; EPR: g_{iso} 1.978 (A_{Mo} 48.6 G).

[Fe(C_5HMe_4)($C_5Me_4CH{=}CHC_5H_4N$)], 6a. To a suspension of [(1′,2,2′,3,3′,4,4′,5-octamethylferrocenyl)methyl]triphenylphosphonium bromide (0.56 g, 1.0 mmol) in dry THF (50 cm^3) cooled to −78 °C was added, in one portion, $KOBu^t$ (0.12 g, 1.1 mmol) and the resulting red mixture was allowed to warm to 0 °C over 1 h. Pyridine-4-carbaldehyde (0.14 cm^3, 0.16 g, 1.5 mmol) was then added and the resulting red mixture stirred at RT for 2 h. Water was added, the mixture extracted with diethyl ether which was dried over Na_2SO_4, filtered and evaporated to dryness *in vacuo*. The residue was chromatographed on alumina using diethyl ether/hexane (1 : 1 v/v) as eluent, giving the product as an orange red solid (mp 130 °C) (0.25 g, 62%). Found: C, 75.1; H, 8.1; N, 3.8. $C_{25}H_{31}FeN$ requires C, 74.8; H, 7.8; N 3.4%. EIMS: *m*/*z* 401 [M^+]; ^{1}H NMR ($CDCl_3$): δ 8.51 (2H, m, C_5H_4N); 7.28 (2H, m, C_5H_4N); 7.12 (1H, d, $^3J_{trans}$ = 16, CH=CH); 6.59 (1H, d, $^3J_{trans}$ = 16, CH=CH); 3.32 (1H, s, C_5HMe_4); 1.65, 1.70, 1.83, 1.99 {24H, each signal 6H, s, $C_5H(CH_3)_4$}; ^{13}C NMR ($CDCl_3$): δ 9.34, 9.89, 11.15, 11.20 (8 × CH_3); 71.45 (CH of C_5HMe_4); 79.91, 80.93, 81.10, 82.77 (other C_5Me_4); 119.75, 123.06, 133.02, 146.11, 150.11 (C_6H_4N and CH=CH).

[Fe(C_5HMe_4){$C_5Me_4CH{=}CHC_5H_4NMo(NO)(Tp^{Me,Me})Cl$}], 6a(Mo). A mixture of **6a** (0.23 g), $[Mo(NO)(Tp^{Me,Me})Cl_2]$ (0.31 g), dry NEt_3 (1 cm^3) in toluene (100 cm^3) was refluxed for 14 h, the mixture then cooled and the solvent evaporated to dryness *in vacuo*. The crude residue was dissolved in the minimum volume of CH_2Cl_2 and chromatographed on silica using CH_2Cl_2 containing THF (1%) as eluant. The product was obtained as a purple solid (0.25 g, 50% yield). Found: C, 55.8; H, 6.5; N, 13.1. Calc. for $C_{40}H_{53}N_8BClOFeMo$: C, 55.9; H, 6.2; N 13.0%. FABMS: *m*/*z* 860 [M^+] 860); IR: 1613 (ν_{NO}), 2545 (ν_{BH}) cm^{-1}; EPR: g_{iso} 1.978 (A_{Mo} = 48.0 G).

[Fe(C_5HMe_4){$C_5Me_4CH{=}CHC_5H_4NMo(NO)(Tp^{Me,Me})Cl$}]-[$PF_6$], [6a(Mo)][$PF_6$]. To a solution of **6a**(**Mo**) (0.2 g) in dry MeCN (50 cm^3) was added ferrocenium hexafluorophosphate (0.08 g) (1 : 1 mole equivalents) and the mixture was sonicated in an ultrasound cleaning bath for 15 min. After evaporation of the solvent the residue was washed several times with diethyl ether until the filtrate was colourless, and the solid was dried *in vacuo* (0.15 g, 85%). Found: C, 44.0; H, 4.5; N, 9.4. $C_{40}H_{53}$-$BClFeF_6N_8MoOP$ requires C, 47.7; H, 5.3; N, 11.1%. FABMS: *m*/*z* 1005 [M^+]; IR (KBr): 1608s (ν_{NO}), 2555w (ν_{BH}), 842 (ν_{PF}) cm^{-1}.

[Fe(C_5HMe_4)($C_5Me_4CH{=}NC_5H_4N$)], 6b. A mixture of 4-aminopyridine (0.38 g, 4 mmol) and $[Al_2Me_6]$ (2 cm^3, 2 M in hexane) in toluene (50 cm^3) was refluxed until gas evolution ceased (*ca.* 30 min). Octamethylferrocene (0.60 g, 1.8 mmol) was then added and the reaction mixture was refluxed for a further 2 h. Water was added, the mixture extracted with diethyl ether and the ether extract evaporated to dryness *in vacuo*. The residue was chromatographed on alumina using CH_2Cl_2 containing NEt_3 (5%) as eluent. The product was isolated as an orange-red solid (0.42 g, 57% yield). Found: C, 70.2; H, 7.3; N, 6.7. $C_{24}H_{30}FeN_2$ requires C, 71.6; H, 7.5; N 7.0%. EIMS: *m*/*z* 402 [M^+]; ^{1}H NMR ($CDCl_3$): δ 8.51 (2H, m, C_5H_4N); 8.36 (1H, s, CH=N); 6.99 (2H, m, C_5H_4N); 3.42 (1H, s, C_5HMe_4); 2.07,

1.85, 1.71, 1.66 {24H, each signal 6H, s, $C_5H(CH_3)_4$}; ^{13}C NMR ($CDCl_3$): δ 9.45, 9.69, 10.44, 11.24 (8 × CH_3); 71.25 (CH of C_5HMe_4); 81.67, 82.34, 85.06 (C_5HMe_4); 115.78, 150.52, 160.89, 165.62 (C_6H_4N and CH=N).

[Fe(C_5HMe_4){C_5Me_4CH=NC_5H_4NMo(NO)($Tp^{Me,Me}$)Cl}], 6b(Mo). A mixture of **6b** (0.25 g), [Mo(NO)($Tp^{Me,Me}$)Cl_2] (0.37 g), and dry NEt_3 (1 cm^3) in toluene (100 cm^3) was refluxed for 14 h. The solvent was then evaporated to dryness *in vacuo* and the crude mixture was purified by chromatography on silica using CH_2Cl_2, hexane (3 : 2 v/v) containing THF (1%) as eluent. The complex was isolated as a purple solid (0.17 g, 32%). Found: C, 56.3; H, 6.7; N, 13.2. $C_{39}H_{52}N_9BClOFeMo$ (with 1 mole THF as solvate) requires C, 55.4; H, 6.5, N, 13.5%. EIMS: *m*/*z* 862 [M^+]; IR 1610 (ν_{NO}), 2548 (ν_{BH}) cm^{-1}; EPR: g_{iso} 1.978 (A_{Mo} = 47.6 G).

[Fe(C_5HMe_4){C_5Me_4CH=C$HC_5H_4NW(CO)_5$}], 6a(W). A solution of [$W(CO)_6$] (0.60 g) in THF (50 cm^3) was photolyzed using a 400W high pressure lamp for 20 min and to the resulting yellow solution **6a** (0.50 g) was added, the reaction mixture being stirred overnight. The solvent was then evaporated *in vacuo*, the excess of [$W(CO)_6$] was sublimed out and the residue dissolved in the minimum volume of hexane and chromatographed on alumina using hexane/diethyl ether (9 : 1 v/v). The product was isolated as an orange solid (0.55 g, 61%). Found: C, 49.8; H, 4.4; N, 1.9. $C_{30}H_{31}NO_5FeW$ requires C, 49.5; H, 4.3; N, 1.9%. FABMS: *m*/*z* 725 [M^+]; IR 2069s, 2069m, 1971m, 1916s, 1886s (all ν_{CO}) cm^{-1}; ^{1}H NMR ($CDCl_3$): δ 8.60–8.63 (2H, m, C_5H_4N); 7.25 (1H, d, $^3J_{trans}$ = 16, CH=CH); 7.2–7.22 (2H, m, C_5H_4N); 6.58 (1H, d, $^3J_{trans}$ = 16, CH=CH); 3.34 (1H, s, C_5HMe_4); 1.64, 1.69, 1.85, 1.99 {24H, each signal 6H, s, $C_5H(CH_3)_4$}; ^{13}C NMR ($CDCl_3$): δ 9.32, 9.87, 11.15, 11.18 (8 × CH_3); 71.60 (CH of C_5HMe_4); 80.44, 81.26, 81.42, 83.09 (C_5HMe_4); 120.21, 120.83, 137.37, 147.38, 155.86 (C_5H_4N and CH=CH); 198.91, 202.58 (CO).

[Fe(C_5HMe_4){C_5Me_4CH=C$HC_5H_4NW(CO)_5$}][PF_6], [6a(W)][PF_6]. To a solution of **6a**(**W**) (0.18 g, 0.25 mmol) in MeCN (50 cm^3) was added ferrocenium hexafluorophosphate (0.08 g, 0.25 mmol) and the mixture was sonicated in an ultrasound cleaning bath for 15 min. After evaporation of the solvent the residue was washed several times with diethyl ether until the filtrate was colourless, and the remaining solid was then dried *in vacuo* (0.16 g, 72%). Found: C, 40.7; H, 3.3; N, 1.4. $C_{30}H_{31}FeF_6NO_5PW$ requires C, 41.4; H, 3.6; N, 1.7%. FABMS: *m*/*z* 725 [$M^+ - PF_6$], 669; IR (KBr): 2070m (ν_{CO}), 1978m (ν_{CO}) 1916s (ν_{CO}), 1873s (ν_{CO}), 841s (ν_{PF}) cm^{-1}.

[Fe(C_5H_5)(C_5H_4N=CHC_5H_4N)], 8. A mixture of ferrocenylamine (0.17 g), 4-pyridinecarbaldehyde (0.15 g) and molecular sieves (0.80 g) was refluxed in freshly distilled methanol (15 cm^3) for 22 h. The mixture was cooled to RT, the dark red precipitate was filtered off, washed with a little dry diethyl ether and dried *in vacuo* giving the product as a red solid (0.07 g, 29%). Found: C, 66.0; H, 5.0; N, 9.7. $C_{16}H_{14}N_2Fe$ requires C, 66.2; H, 4.9; N, 16.8%. EIMS *m*/*z* 290 [M^+]; ^{1}H NMR (CD_2Cl_2): δ 8.67 (2H, m, C_5H_4N); 8.59 (1H, s, CH=N); 7.66 (2H, m, C_5H_4N); 4.65 (2H, t, C_5H_4, *J* = 2.0); 4.35 (2H, t, C_5H_4, *J* = 2.0); 4.19 (5H, s, C_5H_5).

[Fe(C_5H_5)(C_5H_4N=CHC_5H_4N{Mo(NO)($Tp^{Me,Me}$)Cl}], 8(Mo). A mixture of **8** (0.16 g), [Mo(NO)($Tp^{Me,Me}$)Cl_2] (0.31 g) and NEt_3 (1 cm^3) in toluene (60 cm^3) was refluxed overnight, then allowed to cool and evaporated to dryness *in vacuo*. The residue was dissolved in the minimum volume of CH_2Cl_2 and chromatographed on silica. Initial elution with CH_2Cl_2/hexane (9 : 1 v/v) removed traces of unreacted [Mo(NO)($Tp^{Me,Me}$)Cl_2] and [{Mo(NO)($Tp^{Me,Me}$)Cl}$_2$O]. Changing the solvent to CH_2Cl_2 containing THF (1%) allowed elution of the purple compound which was recrystallised from CH_2Cl_2/hexane giving the desired compound as a purple solid (0.14 g, 34%). Found: C, 49.7; H, 5.0; N, 16.6. $C_{31}H_{26}N_8BClOFeMo$ requires C, 49.7; H, 4.9; N, 16.8%. FABMS: *m*/*z* 750 [M^+]; IR 1614 (ν_{NO}); 2536 (ν_{BH}) cm^{-1}; EPR: g_{iso} 1.978 (A_{Mo} = 48.6 G).

[Fe(C_5HMe_4){C_5Me_4CH=CH(C_4H_4S)CH=CHC_5H_4N}], 11. 4-Picoline (0.16 cm^3, 1.60 mmol) in THF (20 cm^3) was added dropwise at −10 °C to a solution of $LiNPr^i_2$ (0.21 cm^3, 1.50 mmol), prepared from diisopropylamine (0.95 cm^3, 1.6M, 1.50 mmol) and $LiBu^n$ (0.16 cm^3, 1.60 mmol). The mixture was then allowed to warm to RT and a solution of **10b** (0.60 g, 1.38 mmol), dissolved in THF (20 cm^3), was added dropwise with stirring over 50 min. The mixture was stirred overnight and then quenched with water (10 cm^3). The product was extracted with CH_2Cl_2, the extract was concentrated *in vacuo*, dried over $MgSO_4$, filtered and evaporated to dryness affording [Fe(C_5HMe_4){C_5Me_4CH=CH(C_4H_4S)CH(OH)$CH_2C_5H_4N$}]. This intermediate alcohol was not further purified but was dissolved in pyridine (10 cm^3) and a solution of $POCl_3$ (0.18 cm^3, 2.00 mmol) in pyridine (10 cm^3) was added dropwise. After stirring at RT for 3 h, the mixture was quenched with water and evaporated to dryness. The residue was suspended in water (50 cm^3) and the mixture made slightly basic with NaOH. Extraction with several portions of CH_2Cl_2, drying over Na_2SO_4, filtration and evaporation to dryness, followed by column chromatography over alumina using ether/hexane (1 : 1 v/v) as eluent, afforded the product as an orange solid (0.37 g, 53%). Found: C, 73.3; H, 7.7; N, 2.8. $C_{31}H_{35}FeNS$ requires C, 73.1; H, 6.9; N, 2.8%. FABMS: *m*/*z* 509 [M^+]; ^{1}H NMR ($CDCl_3$): δ 8.54–8.56 (2H, m, C_5H_4N); 7.39 (1H, d, $^3J_{trans}$ = 16, CH=CH); 7.31–7.33 (2H, m, C_5H_4N); 7.01 (1H, d, *J* = 4, C_4H_2S); 6.83 (1H, d, *J* = 4, C_4H_2S); 6.77 (3H, m, CH=CH); 3.33 (1H, s, C_5HMe_4); 1.97, 1.82, 1.72, 1.67 {24H, each signal 6H, s, $C_5H(CH_3)_4$}; ^{13}C NMR ($CDCl_3$): δ 9.36, 9.91, 11.12, 11.24 (8 × CH_3); 71.49 (CH of C_5HMe_4); 79.58, 81.00, 81.15, 82.46 (C_5HMe_4); 119.15, 120.37, 124.13, 124.27, 126.48, 129.51, 129.62, 138.16, 144.61, 145.98, 150.14 (C_4H_2S, C_5H_4N and CH=CH).

[Fe(C_5HMe_4){C_5Me_4CH=CH(C_4H_2S)CH=C$HC_5H_4NW(CO)_5$}], 11(W). [$W(CO)_6$] (0.50 g) in THF (50 cm^3) was photolyzed with a 400 W high pressure lamp for 20 min. To the resulting yellow solution **11** (0.15 g) was added and the mixture stirred for 4 h. The solvent was evaporated *in vacuo*, the excess of [$W(CO)_6$] sublimed out, and the residue dissolved in the minimum volume of CH_2Cl_2 and the solution column chromatographed and worked up as described above. The product was isolated as an orange solid (0.18 g, 72%). Found: C, 51.8; H, 4.0; N, 1.7. $C_{36}H_{35}NO_5SFeW$ requires C, 51.9; H, 4.2; N, 1.7%. FABMS: *m*/*z* 833 [M^+]; IR 2068m, 1967m, 1900s (ν_{CO}) cm^{-1}; ^{1}H NMR ($CDCl_3$): δ 8.65–8.67 (2H, m, C_5H_4N); 7.43 (1H, d, $^3J_{trans}$ = 16, CH=CH); 7.21–7.26 (2H, m, C_5H_4N); 7.09 (1H, d, *J* = 4, C_4H_2S); 6.86 (1H, d, *J* = 4, C_4H_2S); 6.79 (2H, m, CH=CH); 6.71 (1H, d, $^3J_{trans}$ = 16, CH=CH); 3.34 (1H, s, C_5HMe_4); 1.66, 1.70, 1.82, 1.96 {4H, each signal 6H, s, $C_5H(CH_3)_4$}; ^{13}C NMR ($CDCl_3$): δ 9.35, 9.89, 11.10, 11.21 (8 × CH_3), 71.57 (CH of cp), 79.73, 81.13, 81.27, 82.80 (C_5HMe_4), 118.70, 121.62, 124.44, 129.09, 130.76, 131.37, 137.23, 146.14, 147.60, 155.87 (C_4H_2S, C_5H_4N and CH=CH), 198.86, 202.46 (CO).

[Fe(C_5HMe_4){C_5Me_4CH=CH(C_4H_2S)CH=C$HC_5H_4NW(CO)_5$}][PF_6], [11(W)][PF_6]. To a solution of **11**(**W**) (0.14 g) in MeCN (50 cm^3) was added ferrocenium hexafluorophosphate (0.06 g) and the mixture was sonicated in an ultrasound cleaning bath for 15 min. After evaporation of the solvent the residue was washed several times with diethyl ether until the filtrate was colourless, and the remaining solid was dried *in vacuo* (0.13 g, 81%). Found: C, 45.3; H, 4.5; N, 1.0. Calcd. for $C_{36}H_{35}FeF_6NO_5PSW$: C, 44.2; H, 3.6; N, 1.4%. FABMS: *m*/*z*

Table 1 Crystallographic data for [**1MoCl**]·0.5CH_2Cl_2·0.25C_6H_{14} and [**6a**(**Mo**)][a]

Compound	[**1MoCl**]·0.5CH_2Cl_2·0.25C_6H_{14}	**6a**(**Mo**)
Empirical formula	$C_{27}H_{36.5}BCl_2FeMoN_8O$	$C_{40}H_{53}BClFeMoN_8O$
M	722.64	859.95
Crystal dimensions/mm	0.3 × 0.2 × 0.1	0.3 × 0.1 × 0.05
Crystal system, space group	Triclinic, $P\bar{1}$	Triclinic, $P\bar{1}$
a/Å	11.3036(14)	9.1843(10)
b/Å	12.1739(16)	13.8687(15)
c/Å	23.272(3)	18.0066(19)
α/°	89.163(3)	69.162(2)
β/°	87.426(3)	87.834(2)
γ/°	76.802(3)	71.966(2)
V/Å^3	3114.6(7)	2031.5(4)
Z	4	2
ρ_{calcd}/g cm^{-3}	1.541	1.406
μ/mm^{-1}	1.076	0.774
Reflections collected: total/independent/R_{int}	32882/14154/0.1219	17786/7134/0.0798
Data/restraints/parameters	14154/0/751	7134/0/492
final R_1, wR_2[b,c]	0.0788, 0.2042	0.0535, 0.1157

[a] Data in common: T = 173 K; λ = 0.71073 Å; Bruker SMART-CCD diffractometer. [b] Structure was refined on F_o^2 using all data; the value of R_1 is given for comparison with older refinements based on F_o with a typical threshold of $F \geq 4\sigma(F)$. [c] $wR_2 = [\Sigma[w(F_o^2 - F_c^2)^2]/\Sigma w(F_o^2)^2]^{1/2}$ where $w^{-1} = [\sigma^2(F_o^2) + (aP)^2 + bP]$ and $P = [\max(F_o^2,0) + 2F_c^2]/3$.

833 (M^+). IR 2070m (ν_{CO}), 1978m (ν_{CO}), 1904s (ν_{CO}), 841s (ν_{PF}) cm^{-1}.

[Fe(C_5HMe_4){C_5Me_4CH=$CH(C_4H_2S)CH$=CHC_5H_4NMe}]I, 11(Me$^+$I$^-$). MeI (0.30 g) was added dropwise to a solution of **11** (0.15 g) dissolved in diethyl ether (50 cm^3) and the mixture was stirred overnight. The resulting precipitate was filtered off and washed with ether (×3) giving the product as an orange solid (0.19 g, 97%). Found: C, 59.4; H, 5.7; N, 2.1. $C_{32}H_{38}NISFe$ requires C, 59.0; H, 5.9; N, 2.2%. FABMS: m/z 524 [M^+]; ^{1}H NMR ($CDCl_3$): δ 8.84–8.86 (2H, m, C_5H_4N); 7.89–7.92 (2H, m, C_5H_4N); 7.88 (1H, d, $^3J_{trans}$ = 16, CH=CH); 7.33 (1H, d, J = 4, C_4H_2S); 6.88 (1H, d, J = 4, C_4H_2S); 6.79 (2H, m, CH=CH); 6.74 (1H, d, $^3J_{trans}$ = 16, CH=CH); 4.43 (3H, s, $C_5H_4NCH_3^+$); 3.76 (1H, s, C_5HMe_4); 1.56, 1.59, 1.72, 1.85 {24H, each signal 6H, s, $C_5H(CH_3)_4$}; ^{13}C NMR ($CDCl_3$): δ 9.28, 9.82, 11.07, 11.14 (8 × CH_3); 48.40 (CH_3); 71.67 (CH of C_5HMe_4); 81.22, 83.58, 85.47 (C_5HMe_4); 118.32, 119.00, 122.97, 125.31, 132.84, 135.23, 136.29, 144.35, 150.83, 154.72 (C_4H_2S, C_5H_4N and CH=CH).

X-Ray crystallography

Crystals of **1**(**MoCl**)·0.5CH_2Cl_2·0.25C_6H_{14} and **6a**(**Mo**) were grown by diffusion of hexane into concentrated solutions of the complexes in CH_2Cl_2. In each case a suitable crystal was coated with hydrocarbon oil and attached to the tip of a glass fibre, which was then transferred to a Siemens SMART diffractometer under a stream of cold N_2 at 173 K. Details of the crystal parameters, data collection and refinement for each of the structures are collected in Table 1. After collection of a full sphere of data in each case an empirical absorption correction (SADABS) was applied,[23] and the structures were then solved by conventional direct methods and refined on all F^2 data using the SHELX suite of programs.[24] In all cases, non-hydrogen atoms were refined with anisotropic thermal parameters; hydrogen atoms were included in calculated positions and refined with isotropic thermal parameters.

For [**1MoCl**]·0.5CH_2Cl_2·0.25C_6H_{14}, the asymmetric unit contains two independent complex molecules, one molecule of CH_2Cl_2, and one half of a hexane molecule (adjacent to an inversion centre). Hydrogen atoms were not included in the refinement for these solvent molecules. Selected bond lengths and angles for the two structures are collected in Tables 2 and 3.

CCDC reference numbers 165091 and 165092.

See http://www.rsc.org/suppdata/dt/b1/b104791b/ for crystallographic data in CIF or other electronic format.

Results and discussion

Synthesis and characterisation

The compounds investigated in this work are summarised in Scheme 1, and fall into three general classes: a group of complexes in which a deprotonated ferrocenyl–amine ligand is coordinated to the 16-valence electron centre {M(NO)($Tp^{Me,Me}$)-X} (M = Mo, X = Cl, Br or I; M = W, X = Cl), *viz.* series **1**, **2** and **3**; a similar group containing ferrocenyl–pyridines bound to the 17-valence electron moiety {Mo(NO)($Tp^{Me,Me}$)Cl}, *viz.* **4**(**MoCl**)–**9**(**Mo**), or to a {$W(CO)_5$} moiety, **6a**(**W**); and a few other compounds based on dipolar organic species containing octamethylferrocene connected to a variety of organic and inorganic acceptor units, *viz.* **10** and **11**. The synthesis and characterisation of **2**(**MoCl**) and all of series **3**, **4**, **7**, **9** and **10** have already been reported.[7,13,21]

The complexes of series **1** are new, being obtained by reaction of ferrocenylamine[11] with [Mo(NO)($Tp^{Me,Me}$)X_2] in the presence of NEt_3 in toluene, the base being necessary to remove HX generated in the reaction. These complexes are either green (Mo) or deep blue (W). The anilido compound **2**(**MoBr**) was obtained similarly, using 4-ferrocenylaniline. The pyridyl complexes, some of which are derived from previously unreported permethylated ferrocenyl derivatives (see Experimental section) were obtained by reaction of the ferrocenylpyridine ligand with [Mo(NO)($Tp^{Me,Me}$)Cl_2], also in the presence of NEt_3 which functions as a reducing agent (Mo^{II} is reduced to Mo^{I} as a chloride ligand is replaced by a pyridyl ligand). The tungsten carbonyl complexes **6a**(**W**) and **11**(**W**) were obtained by reaction of the appropriate ferrocenylpyridine ligand with [$W(CO)_5$(THF)], which was generated photolytically from [$W(CO)_6$] in THF. **11**(**Me$^+$I$^-$**) was prepared by addition of methyl iodide in diethyl ether to **11**. All new compounds were characterised satisfactorily by elemental analyses, ^{1}H NMR spectroscopy (where diamagnetic), EPR spectroscopy (where paramagnetic) and FAB mass spectrometry. The crystal structures of **1**(**MoCl**) and **6a**(**Mo**) were determined crystallographically and are reported below. The structures of **10a** and [**10a**][PF_6] were described by us recently in a preliminary communication.[21]

The ^{1}H NMR spectra of series **1** and of **2**(**MoBr**) were unremarkable, all exhibiting a resonance in the region δ 10–13 due to the NH group bound to the electron-deficient metal nitrosyl centre as previously noted in **2**(**MoCl**) and **2**(**MoBr**), and in other alkyl amido and anilido complexes.[10,25] The paramagnetic species **5**(**Mo**), **6a**(**Mo**), **6b**(**Mo**) and **8**(**Mo**) showed

Table 2 Selected bond lengths (Å) and angles (°) for **[1MoCl]**·$0.5CH_2Cl_2$·$0.25C_6H_{14}$

Mo(1)–N(2)	1.775(7)	Mo(2)–N(10)	1.758(8)
Mo(1)–N(1)	1.946(7)	Mo(2)–N(9)	1.945(7)
Mo(1)–N(3)	2.157(7)	Mo(2)–N(13)	2.177(7)
Mo(1)–N(5)	2.225(7)	Mo(2)–N(15)	2.226(7)
Mo(1)–N(7)	2.238(7)	Mo(2)–N(11)	2.252(7)
Mo(1)–Cl(1)	2.430(2)	Mo(2)–Cl(2)	2.438(2)
N(2)–Mo(1)–N(1)	95.7(3)	N(10)–Mo(2)–N(9)	96.3(3)
N(2)–Mo(1)–N(3)	94.8(3)	N(10)–Mo(2)–N(13)	94.3(3)
N(1)–Mo(1)–N(3)	92.8(3)	N(9)–Mo(2)–N(13)	93.6(3)
N(2)–Mo(1)–N(5)	95.0(3)	N(10)–Mo(2)–N(15)	92.9(3)
N(1)–Mo(1)–N(5)	167.4(3)	N(9)–Mo(2)–N(15)	168.9(3)
N(3)–Mo(1)–N(5)	79.6(3)	N(13)–Mo(2)–N(15)	79.6(3)
N(2)–Mo(1)–N(7)	179.5(3)	N(10)–Mo(2)–N(11)	177.5(3)
N(1)–Mo(1)–N(7)	84.1(3)	N(9)–Mo(2)–N(11)	86.1(3)
N(3)–Mo(1)–N(7)	84.8(3)	N(13)–Mo(2)–N(11)	84.9(3)
N(5)–Mo(1)–N(7)	85.2(2)	N(15)–Mo(2)–N(11)	84.6(3)
N(2)–Mo(1)–Cl(1)	92.1(2)	N(10)–Mo(2)–Cl(2)	92.2(3)
N(1)–Mo(1)–Cl(1)	99.6(2)	N(9)–Mo(2)–Cl(2)	98.2(2)
N(3)–Mo(1)–Cl(1)	165.09(19)	N(13)–Mo(2)–Cl(2)	165.8(2)
N(5)–Mo(1)–Cl(1)	86.71(19)	N(15)–Mo(2)–Cl(2)	87.51(19)
N(7)–Mo(1)–Cl(1)	88.28(19)	N(11)–Mo(2)–Cl(2)	88.02(19)

Table 3 Selected bond lengths (Å) and angles (°) for **6a**(**Mo**)

Mo(1)–N(100)	1.886(6)
Mo(1)–N(4)	2.168(4)
Mo(1)–N(6)	2.185(4)
Mo(1)–N(31)	2.193(4)
Mo(1)–N(1)	2.229(4)
Mo(1)–Cl(1)	2.4353(18)
N(100)–Mo(1)–N(4)	95.68(18)
N(100)–Mo(1)–N(6)	94.17(18)
N(4)–Mo(1)–N(6)	83.28(15)
N(100)–Mo(1)–N(31)	90.29(18)
N(4)–Mo(1)–N(31)	172.19(16)
N(6)–Mo(1)–N(31)	91.29(15)
N(100)–Mo(1)–N(1)	177.3(2)
N(4)–Mo(1)–N(1)	86.68(16)
N(6)–Mo(1)–N(1)	84.75(15)
N(31)–Mo(1)–N(1)	87.24(15)
N(100)–Mo(1)–Cl(1)	93.54(16)
N(4)–Mo(1)–Cl(1)	91.51(11)
N(6)–Mo(1)–Cl(1)	171.09(11)
N(31)–Mo(1)–Cl(1)	93.14(11)
N(1)–Mo(1)–Cl(1)	87.74(12)

characteristic isotropic EPR spectra in solution (a six-line multiplet imposed on a strong singlet, arising from two sets of Mo isotopes with $I = 5/2$ and $I = 0$ respectively), the values of g_{iso} (1.978) and A_{iso} (*ca.* 4.9 mT) being essentially identical to those of **4**(**MoCl**), **7**(**Mo**) and **9**(**Mo**).[13]

The NO stretching frequency of the nitrosyl complexes occurred in the expected regions, being mainly a function of the metal centre and on whether it has a 16- or 17-valence electron configuration. The series **1** complexes exhibited ν_{NO} at *ca.* 1642 cm^{-1} (Mo) and *ca.* 1614 cm^{-1} (W), these values being *ca.* 10 cm^{-1} lower than in series **2** where there is an additional phenylene spacer separating the metal centres. This change in ν_{NO} reflects the relative proximity of the electron-rich ferrocenyl group to the nitrosyl acceptor in the former compared to the latter species. The {$W(CO)_5$} derivatives exhibited characteristic CO stretching frequencies between 2100 and 1880 cm^{-1}.

Crystal structures

The 16-valence electron complex **1**(**MoCl**) crystallises in the centrosymmetric space group $P\bar{1}$, with two independent molecules in the asymmetric unit. The molybdenum atom is six-coordinate, with few significant distortions and the Mo–N–O bond angle is essentially linear, as expected. The structure is shown in Fig. 1 and the important bond lengths and angles are

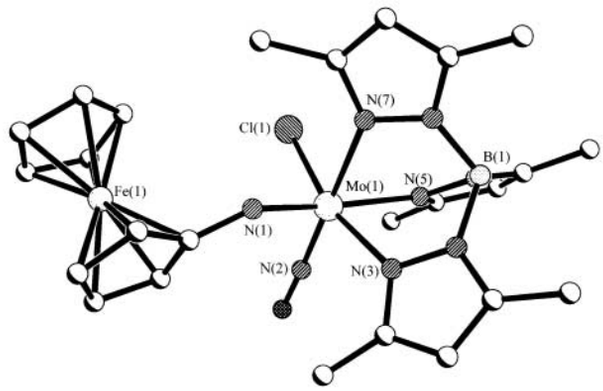

Fig. 1 Molecular structure of **1**(**MoCl**).

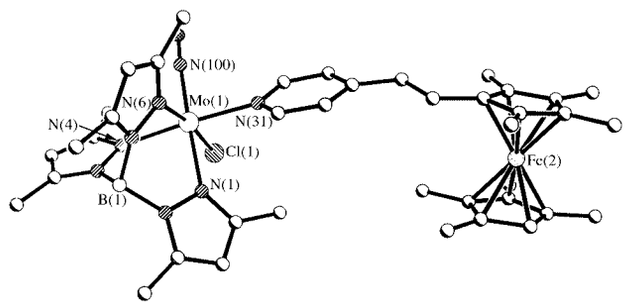

Fig. 2 Molecular structure of **6a**(**MoCl**).

listed in Table 2. These data show clearly that the Mo–N(amide) bond is short [1.945(7) and 1.946(7) Å in the two independent molecules] and that the stereochemistry around the N(1){N(9)} atom is planar, consistent with sp^2 hybridisation, as expected.[25] These observations are entirely consistent with significant $N(p_z) \longrightarrow Mo(d_{xy})$ π-donation, an important manifestation of the polarising power of this class of coordinatively unsaturated, electron-deficient metal nitrosyl complex. There are no significant intra- or inter-molecular contacts, the Fe(1) · · · Mo(1) and Fe(2) · · · Mo(2) distances being 4.63 and 4.64 Å, respectively.

The 17-valence electron complex **6a**(**Mo**) also crystallised in the centrosymmetric space group $P\bar{1}$. Again, the metal atom is pseudo-octahedral and the Mo–N–O bond angle is near linear. The structure is shown in Fig. 2 and the important bond lengths and angles are listed in Table 3. The $C_5H_4CH{=}CHC_5H_4N$ linker group is somewhat distorted from planarity, with the plane of the pyridyl ring being 20° out of the plane of the cyclopentadienyl ring to which it is attached. The orientation of the pyridyl ring at the Mo centre appears, as usual, to be dictated largely by steric interactions with the pyrazolyl methyl groups, with the plane of the pyridyl ring being very close (5.4°) to that of the pyrazolyl ring opposite it. If the Mo–NO axis is taken as the *z* direction, then the *xy* plane is described by N(4), N(6), N(31) and Cl(1), and the pyridyl ring is oriented at 45° to this plane. This allows substantial (but clearly not maximal) overlap between the SOMO (d_{xy}) and the π-orbitals of the pyridyl ring.[26]

Electrochemical properties

The electrochemical behaviour of the new complexes conform to the behaviour of similar species which we have described before,[6] and the data are collected in Table 4. Those derivatives containing the {$Fe(C_5H_4{-})(C_5H_5)$} group exhibited characteristic oxidation behaviour at potentials very close to that of the internal reference ferrocene, reducing to *ca.* −0.2 V for {$Fe(C_5H_4{-})(C_5Me_5)$} and to −0.3 V for {$Fe(C_5Me_4{-})(C_5Me_4H)$} fragments. Attachment of the electronegative 16- or 17-valence electron {$M(NO)(Tp^{Me,Me})$} fragments, however, does not appear to have much effect on the redox potential of

Table 4 Electrochemical data in CH_2Cl_2

Compound	E_f/V (ΔE_p/mV)[a]		
	Reduction	Oxidation	
	Mo/W	Ferrocenyl	Mo/W
1(MoCl)	−1.68 (110)	−0.02 (80)	
1(MoBr)	−1.64 (90)	−0.01 (90)	
1(MoI)	−1.60[c]	0.00 (90)	
1(WCl)	−2.06 (120)	−0.12 (90)	
2(MoCl)[b]	−1.39	+0.02	
2(MoBr)	−1.39 (90)	+0.02 (80)	
2(MoI)[b]	−1.35[c]	+0.02	
2(WCl)[b]	−1.80	−0.01	
3a[b]	−1.31	+0.01	
3b[b]	−1.14	+0.06	
4(MoCl)[b]	−1.94	+0.10	+0.01
4(MoI)	−1.84 (110)		+0.06 (120)[f]
5(Mo)	−2.01 (140)	−0.18 (90)	+0.01 (80)
6a(Mo)	−2.01 (130)	−0.31 (80)	+0.01 (70)
6b(Mo)	−2.02 (120)	−0.16 (80)	+0.02 (70)
6a(W)		−0.30 (90)	+0.67[c,e]
7[b]		+0.04	+0.16[e]
7(Mo)[b]	−1.47	+0.08	+0.02
8(Mo)	−1.70 (120)		+0.07 (170)[f]
9[b]		+0.03	
9(Mo)[b]	−1.86		+0.04[f]
11	−2.32[c,d]	−0.36 (90)	
11(W)	−1.98 (80)[d]	−0.37 (90)	+0.64[c,d]

[a] All measurements are made in CH_2Cl_2 containing 0.1 M $[NBu^n_4][PF_6]$ at a Pt working electrode; all potentials are *vs.* the ferrocene/ferrocenium couple. [b] Previously-published data; see refs. 7, 13 and 21. [c] Irreversible process. [d] Reduction of the bis(alkenyl)thiophenyl group. [e] Unidentified oxidation process, possibly associated with $\{W(CO)_5\}$ fragment. [f] Two overlapping one-electron oxidations which could not be resolved.

the ferrocenyl groups. The difference between the ferrocenyl redox potentials in **6b(Mo)** (−0.16 V) and **6a(Mo)** (−0.31 V) presumably reflects the electronegativity of the N atom in the azomethine link relative to C in the alkene bridge; similar behaviour (although to a lesser extent) occurring in the pair **3a** and **3b**.

Those complexes containing the 16-valence electron $\{M(NO)(Tp^{Me,Me})\}^{2+}$ moiety, *e.g.* series **1**, **2**, and **3**, exhibit a one-electron reduction (formally a M^{II}/M^{I} couple) corresponding to the formation of a 17-valence electron monoanion, $[Fc–bridge–\{M(NO)(Tp^{Me,Me})X\}]^-$. This is entirely characteristic of these fragments and the variation in redox potential with metal and co-ligand are in agreement with our previous observations.[6] Reduction of the iodo complexes, *i.e.* **1(MoI)** and **2(MoI)**, is irreversible because of dissociation of I^- in the reduced state and the concomitant formation of new electroactive species,[27] this behaviour obviously affecting attempts to study the reduced species spectroscopically. These M^{II}/M^{I} couples are at more negative potentials for the series **1** complexes than for those of series **2** and **3**, indicating that the closer the donor ferrocenyl group is to the $\{M(NO)(Tp^{Me,Me})\}$ fragment, the more electron-rich that fragment becomes, making it harder to reduce.

The molybdenum nitrosyl complexes containing 17-valence electron cores, *viz.* **4(Mo)**–**9(Mo)**, reduce in a one-electron step and oxidise in two sequential one-electron steps: formally Mo^{I}/Mo^{0}, Mo^{II}/Mo^{I} and Fc^+/Fc couples, respectively. The redox potentials of the Mo^{I}/Mo^{0} couples are in the range −1.80 to −2.01 V, consistent with the formation of a 18-valence electron $\{Mo(NO)(Tp^{Me,Me})Cl\}^-$ fragment, and appear to be influenced by the extent of methylation of the ferrocenyl rings, *i.e.* the relative electron-richness of the donor group. On the other hand, the Mo^{II}/Mo^{I} redox potentials are virtually unaffected by the nature of the ferrocenyl group, and all occur close to 0.0 V *vs.* Fc/Fc^+, *i.e.* close to the ferrocene/ferrocenium couple. This difference between the sensitivity of the Mo^{I}/Mo^{0} and Mo^{II}/Mo^{I} couples in relation to the nature of substituents on the pyridyl ligand has been noted before.[13,28] It arises from a decrease in the energy of the singly occupied molecular orbital [which is largely metal-based (d_{xy})] on oxidation, thereby reducing its interaction with the π-acceptor pyridyl ligand. The opposite happens when the $\{Mo(NO)(Tp^{Me,Me})Cl\}$ fragment is reduced, the overlap between the d_{xy} orbital and the pyridyl π-orbitals increasing significantly, leading to marked dependence of the reduction potentials of **4(Mo)**–**9(Mo)** on the nature of the substituent on the pyridyl ring, *i.e.* the ferrocenyl unit.

The complexes **6a(W)** and **11(W)** are also redox-active. The cyclic and square wave voltammograms of the former show oxidation of the octamethylferrocenyl group at a potential 70 mV more positive than that of the latter, implying that the additional conjugated alkenyl–thienyl spacer in the latter case significantly raises the HOMO of the ferrocenyl group. Both complexes undergo an irreversible oxidation at *ca.* +0.65 V, possibly associated with the $\{W(CO)_5\}$ fragment, but only **11(W)** is reduced at *ca.* −2.0 V, a process seemingly associated with the bis(alkenyl)thiophenyl group.

Electronic spectra

The electronic spectral data of all complexes discussed in this paper are presented in Table 5. Since all of them contain a substituted ferrocenyl moiety, it is appropriate to comment first on the contribution of this group to the overall electronic spectral picture. The lowest energy transition of the ferrocenyl unit occurs in the region 400–500 nm, with intensities ranging from 1000 to 5000 $dm^3\ mol^{-1}\ cm^{-1}$, and has a mixture of d–d and Fe⟶(substituted)Cp metal-to-ligand charge-transfer (MLCT) character. The second lowest energy transition also has some d–d character, mixed with ligand centred π⟶π* character from the substituted cyclopentadienyl unit; it being accordingly sensitive to the nature of the side chain. Two more intense transitions at higher energy also have some MLCT character.

The low-energy spectra of simple 16-valence electron anilido complexes $[M^{II}(NO)(Tp^{Me,Me})X(NHAr)]$ have an ArNH⟶M ligand-to-metal charge transfer (LMCT) transition which normally falls in the region 490–530 nm.[10] This is usually quite intense (ε 5000–10000 $dm^3\ mol^{-1}\ cm^{-1}$), its position being determined mainly by M but also by X, becoming red-shifted either as its electronegativity decreases and/or its π-donor ability increases. It is clear that this band will overlap substantially with the lowest-energy transition of the ferrocenyl unit, rendering assignment of absorption maxima (which may be the sum of many closely-spaced components from different chromophores) difficult. Despite this *caveat* the spectra of **2** do broadly conform to this pattern, although the LMCT absorptions are at lower energy, falling between 590 and 630 nm for the Mo complexes, and at 510 nm for **2(WCl)**. This decrease in energy reflects the increased donor character (higher energy HOMO) of the ferrocenyl group in series **2** relative to other more simple substituents. The FcNH⟶M LMCT bands in series **1**, while also conforming to the general effects of M and X, occur at even lower energies than in series **2**, at 730–770 nm for the Mo species and at 589 nm for **1(WCl)**. The presence of a low-energy charge-excited state which (i) will involve a substantial degree of charge transfer from one end of the complex to the other, and (ii) has a high intensity indicating that the transition is strongly allowed, suggests that these complexes are well designed from the point of view of achieving significant values of β. In contrast, the LMCT absorptions in **3** are at considerably higher energy than those in **2**, reflecting the lower energy HOMO in the former case and consequently less effective electron-donating behaviour.

The electronic spectra of 17-valence electron pyridine complexes $[Mo(NO)(Tp^{Me,Me})Cl(pyR)]$ usually contain two bands

Table 5 Electronic spectra in CH_2Cl_2 of complexes in different oxidation states, from spectroelectrochemical measurements at −30 °C

Compounds	λ_{max}/nm ($\varepsilon \times 10^{-3}$ mol^{-1} cm^{-1})				
1(MoCl)	282 (6.9)		421 (11.6)		737 (3.9)
[1(MoCl)]$^+$	277 (15.0)		443 (13.5)		864 (1.2)
[1(MoCl)]$^-$	295 (8.4)	362 (8.1)		528 (6.9)	
1(MoBr)		315 (7.4)	432 (11.5)		753 (4.0)
[1(MoBr)]$^+$	284 (10.3)	373 (6.8)	454 (10.8)		789 (1.3)
[1(MoBr)]$^-$	299 (5.3)	386 (5.3)		533 (5.8)	
1(MoI)		369 (8.4)	439 (9.4)		764 (3.9)
[1(MoI)]$^+$	278 (9.5)		442 (10.7)	507 (7.6)	803 (1.2)
1(WCl)		368 (11.0)		589 (3.4)	
[1(WCl)]$^+$	279 (11.9)	395 (10.6)	462 (6.8)		
[1(WCl)]$^-$		364 (6.0)		529 (5.5)	
2(MoCl)	287 (14.1)		470 (14.0)	596 (8.3)	
[2(MoCl)]$^+$	287 (17.4)		480 (20.4)		939 (1.8)
[2(MoCl)]$^-$	305 (11.8)	344 (10.3)	434 (14.3)		
2(MoBr)	292 (11.6)		474 (12.4)		609 (7.3)
[2(MoBr)]$^+$			484 (16.8)		943 (1.5)
[2(MoBr)]$^-$	307 (10.5)	339 (9.0)	437 (11.7)	593 (2.4)	
2(MoI)	294 (12.4)		488 (13.4)		627 (8.0)
2(WCl)	243 (17.8)	277 (10.3)	408 (8.6)	510 (4.4)	
3a	295 (14.9)	341 (24.0)		530 (19.2)	
[3a]$^+$		329 (22.2)		514 (25.4)	955 (1.7)
[3a]$^-$	294 (11.6)	393 (16.0)	477 (26.8)	525 (34.5)	
3b		362 (13.0)	479 (19.0)	580sh	
[3b]$^+$	299 (12.9)	347 (12.9)	494 (22.5)		806 (1.4)
[3b]$^-$			572 (16.0)	618 (17.8)	1064 (0.7)
4	266 (10.3)	314 (17.8)	371 (2.4)	466 (1.5)	
4(MoCl)	276 (14.0)	328 (21.0)		511 (5.7)	
[4(MoCl)]$^+$		346 (17.6)	397 (10.0)	514 (10.0)	1064 (1.6)
[4(MoCl)]$^{2+}$	240 (23.7)	307 (23.9)	439 (14.8)		771 (0.7)
[4(MoCl)]$^-$	255 (15.5)	376 (10.5)	442 (9.8)		926 (21.7)
[4(MoI)]	273 (13.8)	332 (21.6)		516 (6.0)	
5	278 (13.6)	326 (18.2)	388 (2.7)	489 (2.9)	
5(Mo)	280 (15.9)	353 (19.5)	408 (7.7)	547 (8.2)	
[5(Mo)]$^+$	267 (21.4)	321 (22.0)		564 (2.6)	862 (0.6)
[5(Mo)]$^{2+}$	266 (22.1)	327 (23.1)	466 (13.3)		817 (1.0)
[5(Mo)]$^-$		348 (8.9)	387 (10.0)	442 (9.5)	934 (17.0)
6a	276 (26.7)	334 (33.3)		503 (4.4)	
6a(Mo)	277 (10.5)	367 (14.4)		555 (4.5)	
[6a(Mo)]$^+$		322 (21.2)	380 (23.4)	589 (1.7)	
[6a(Mo)]$^{2+}$	273 (15.7)	328 (20.3)	380 (8.1)	464 (8.3)	
[6a(Mo)]$^-$		385 (6.4)	394 (5.6)	432 (5.4)	946 (17.2)
6a(W)		393 (24.0)		552 (4.8)	
[6a(W)]$^+$	293 (20.7)	325 (20.6)	402 (10.5)		
6b	261 (15.5)	319 (13.0)		503 (1.8)	
6b(Mo)	277 (16.8)	341 (14.6)		532 (3.7)	
[7(Mo)]	283 (15.3)	336 (6.2)		570 (2.0)	
[7(Mo)]$^+$	273 (15.3)	351 (5.0)	395 (3.8)	568 (1.9)	
[7(Mo)]$^{2+}$		307 (7.5)	401 (5.2)		753 (0.3)
[7(Mo)]$^-$		422 (2.4)		530 (3.0)	807 (4.8)
8	277 (15.3)	334 (11.9)		569 (5.3)	
8(Mo)	278 (15.3)	335 (11.9)		570 (5.3)	
[8(Mo)]$^+$	280 (13.7)	342 (11.8)	410 (11.8)	572 (3.6)	
[8(Mo)]$^{2+}$	234 (25.8)	296 (18.8)	404 (13.3)		731 (0.7)
[8(Mo)]$^-$		388 (6.7)	445 (9.2)	507 (7.5)	776 (18.3)
9(Mo)	278 (6.2)	355 (11.0)	495 (3.1)	569 (1.0sh)	
[9(Mo)]$^+$	277 (6.5)	360 (10.0)		500 (3.5)	848 (0.3)
[9(Mo)]$^{2+}$		343 (10.6)	400 (7.6)	502 (5.2)	814 (0.4)
[9(Mo)]$^-$	276 (6.2)	305 (4.1)	473 (7.3)		933 (10.7)
10a			451 (14.2)		646 (4.7)
[10a]$^+$	283 (13.1)	387 (14.2)		563 (4.3)	
10b	255 (13.8)	397 (18.7)			
11		314 (11.9)	410 (31.0)	538 (6.5)	709 (9.3)
11(Me$^+$I$^-$)		355 (11.5)		515 (31.1)	
11(W)			444 (27.4)	571 (6.3)	
[11(W)]$^+$		407 (39.7)	463 (36.1)		

between 400 and 500 nm.[29] These have MLCT character, where the acceptor orbital is the LUMO of the pyridine ligand, and they overlap the MLCT bands of the ferrocenyl ligands thus again making assignments of the spectra of the molybdenum nitrosyl complexes **4(Mo)**–**9(Mo)** difficult. However, comparison of the electronic spectra of the free ferrocenyl–pyridine ligands with those of their molybdenated analogues shows that the lowest energy MLCT transition of the ferrocenyl–pyridine ligands shifts at least 50 nm into the red on attachment of the {Mo(NO)($Tp^{Me,Me}$)Cl} units, showing that this {Mo(NO)($Tp^{Me,Me}$Cl} group is electronegative, as we have noted before.[13]

The lowest energy transition in **10a** is lower than that in **10b** consistent with the more effective acceptor ability of the NO_2 group. The comparable transition in **11** is lower still, indicating the powerful delocalising effect of the thienyl group. Similar to the effect of the {Mo(NO)($Tp^{Me,Me}$)Cl} fragment, attachment of {$W(CO)_5$} to the ligand **9** causes a 50 nm red-shift of the lowest energy ferrocenyl MLCT transition, and the same effect

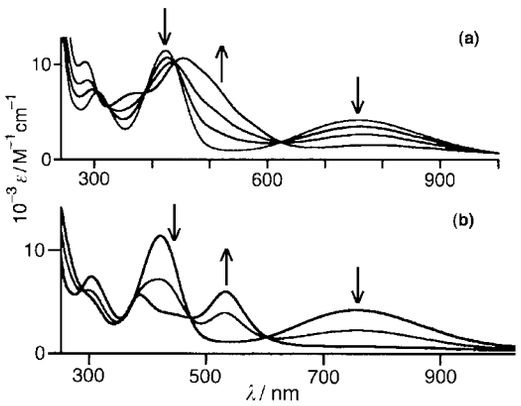

Fig. 3 Electronic spectra recorded during (a) oxidation of **1**(**MoBr**) to [**1**(**MoBr**)]$^+$, and (b) reduction of **1**(**MoBr**) to [**1**(**MoBr**)]$^-$ recorded in an OTTLE cell (CH_2Cl_2, 243 K).

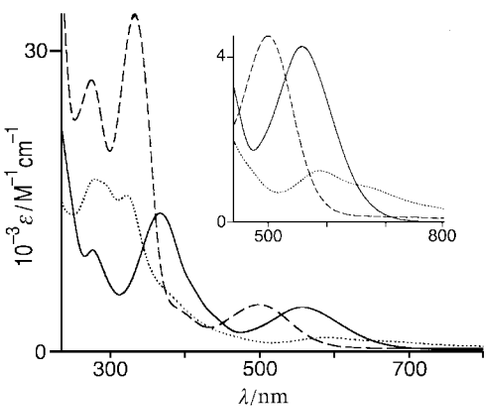

Fig. 4 Electronic spectra of **4** (dashed line), **4**(**MoCl**) (solid line) and [**4**(**MoCl**)]$^+$ (dotted line) (CH_2Cl_2, 243 K).

is seen by comparison of **11** with **11**(**W**). Surprisingly, however, methylation of the pendant pyridyl unit of **11** to give **11**(**Me$^+$I$^-$**) results in the loss of the low-energy absorption at 709 nm, a new absorption appearing at 515 nm.

Finally, we note that the low-energy transitions in all of the complexes discussed here are solvatochromic,[13] the effects in the 16-valence electron metal nitrosyl complexes being more substantial than those in the 17-valence electron species, suggesting that the former are more polarisable than the latter.

Spectroelectrochemical studies

UV/VIS/NIR spectroelectrochemical measurements were carried out on the complexes in all accessible oxidation states, using dichloromethane as the solvent at −30 °C. The data are summarised in Table 5 and the spectral behaviour of **1**(**MoBr**), **4** and **4**(**MoCl**) is shown in Fig. 3 and 4. Because the two chromophores in these complexes have spectral features which overlap at the higher-energy end of the spectrum, assignment of the spectral changes in different oxidation states in this region has not been attempted. However there are a few cases where characteristic low-energy transitions can be identified which are clearly associated with one chromophore, and the behaviour of these during the redox changes is more obvious.

Oxidation of **1**(**MoCl**), **1**(**MoBr**) and **1**(**MoI**), which is associated with the ferrocenyl group, causes the FcNH⟶Mo LMCT to be replaced by a weaker transition (about one-third of the intensity of the original LMCT transition) at lower energy (800 nm region). This cannot still have FcNH⟶Mo LMCT character as such a transition would be blue-shifted by oxidation of the ferrocenyl unit, so this new transition is more likely to be based on the ferrocenium unit. The unsubstituted ferrocenium cation has a weak transition at *ca.* 850 nm which is probably a mixture of (Cp^-)⟶Fe(III) LMCT and d–d character.[30] The presence of an electron-rich (formally uninegative) amido substituent on the ferrocenium unit would enhance the LMCT character of this transition, accounting for its intensity. Similar behaviour is observed on oxidising the complexes of series **2** and **3**: the ferrocenium-based d–d/LMCT absorption appears at *ca.* 940 nm in [**2**(**MoCl**)]$^+$ and [**2**(**MoBr**)]$^+$, at 955 in [**3a**]$^+$, and at 806 nm in [**3b**]$^+$. A similar absorption, however, could not be detected in the spectrum of [**1**(**WCl**)]$^+$, something for which we have no explanation.

One-electron reduction of the amido complex series **1**–**3** results in disappearance of the ArNH⟶M LMCT transition as the metal attains an 18-electron configuration. For [**1**(**MoCl**)]$^-$ and [**1**(**MoBr**)]$^-$ a new stronger transition appears in the region 500–540 nm whose nature is unclear. This transition does not appear for [**1**(**WCl**)]$^-$, [**2**(**MoCl**)]$^-$ or [**2**(**MoBr**)]$^-$, possibly because it occurs at higher energy and therefore overlaps with charge transfer bands associated with the ferrocenyl unit. It is, however, also apparent on reduction of **3a**. Although the ArNH⟶Mo LMCT transition at 530 nm should disappear when the metal is reduced to an 18-electron confuguration, it is apparently replaced by two more intense transitions, one at about the same energy (525 nm) and another at 477 nm, and we assume that this is related to the new transition in the same region which we observed for [**1**(**MoCl**)]$^-$ and [**1**(**MoBr**)]$^-$. It was not possible to obtain spectra from [**1**(**MoI**)]$^-$ because the reduced complex is unstable, as mentioned earlier.

We have previously observed that oxidation of [Mo(NO)(Tp^{Me,Me})Cl(py)], in which the unique electron is lost from the d_{xy} orbital (SOMO), results in the appearance of two new transitions: a weak one at 776 nm, probably largely of d–d character, and a strong one at 407 nm which is a mixture of several LMCT processes to the oxidised metal centre.[29] This Mo^{II}/Mo^{I} couple tends to be close to the position of the ferrocene/ferrocenium couple. Oxidation of **4**(**MoCl**) occurs in two steps, one clearly associated with the ferrocene and the other with the molybdenum nitrosyl centre, but the two are close together and it is not immediately obvious which one is which. The first oxidation causes the appearance of a new absorption at 1064 nm which seems too strong ($\varepsilon = 1{,}600$ dm^3 mol^{-1} cm^{-1}) for a d–d transition but is consistent, however, with an LMCT process associated with the oxidised ferrocenium unit. The second oxidation causes this near-infrared band to be blue-shifted to 770 nm and reduced in intensity. We expect the ferrocenium-based LMCT transition to persist when the Mo centre is oxidised, but given the involvement of the conjugated side-arm in the ferrocenium-based LMCT process, oxidation of the Mo fragment would be expected to move this transition to higher energy, as observed. Coincidentally, we expect the weak d–d transition of the oxidised Mo centre to be in the same region so it is not resolved, but from the spectra we suggest that for **4**(**MoCl**) the ferrocenyl unit oxidises first and the Mo unit second.

From the evolution of the spectra of **5**(**Mo**) and **9**(**Mo**) on oxidation it is not clear which metal-containing component oxidises first and which second. In each case a weak transition appears in the 800–900 nm region following one-electron oxidation, which could plausibly be assigned as either ferrocenium-based LMCT or Mo-based d–d, and this does not change much following the second oxidation. However, in **5**(**Mo**) the redox potential of the ferrocene/ferrocenium couple is expected to be at a quite negative potential due to the methyl substituents on the ferrocene unit, so in this case it seems clear that the first oxidation is ferrocene-based (at −0.18 V) and the second is Mo-based (at +0.01 V *vs.* Fc/Fc$^+$). The peak in the 800–900 nm region which appears in the oxidised forms of **5**(**Mo**) is therefore ferrocenium-based LMCT. Comparison with the spectra of the oxidised forms of **9**(**Mo**) suggests that in this complex the oxidations again occur in the same sequence, with the transition at 848 nm in the spectrum of [**9**(**Mo**)]$^+$ being assigned as a ferrocenium-based LMCT.

Table 6 Linear optical and quadratic nonlinear optical response parameters[a]

Compound	λ_{max}/nm ($10^{-3}\varepsilon$/dm^3 mol^{-1} cm^{-1})	$\beta^b/10^{-30}$ esu	$\beta_o{}^c/10^{-30}$ esu
1(MoCl)	737 (3.9)	119 ± 12	57 ± 6
1(MoBr)	753 (4.0)	135 ± 14	67 ± 7
1(MoI)	764 (3.9)	197 ± 29	101 ± 10
1(WCl)	589 (3.4)	240 ± 24	38 ± 4
2(MoCl)	596 (8.3)	297 ± 30	52 ± 5
2(MoBr)	609 (7.3)	289 ± 29	60 ± 6
2(MoI)	627 (8.0)	431 ± 43	110 ± 11
2(WCl)	510 (4.4)	56 ± 8	4 ± 0.6
3a	530 (19.2)	975 ± 98	3 ± 0.3
3b	479 (19.0)	564 ± 56	85 ± 9
4	466 (1.5)	16 ± 2	3 ± 0.5
4(MoCl)	511 (5.7)	42 ± 6	3 ± 0.45
4(MoI)	516 (6.0)	36 ± 6	2 ± 0.3
5	489 (2.9)	73 ± 11	9 ± 1
5(Mo)	547 (8.2)	177 ± 18	8 ± 1
6a	503 (4.4)	76 ± 11	6 ± 1
6a(Mo)	555 (4.5)	205 ± 21	14 ± 2
[6a(Mo)]$^+$	589 (1.6)	129 ± 13	20 ± 2
6a(W)	552 (4.8)	252 ± 25	14 ± 2
[6a(W)]$^+$	402 (10.5)	[d]	[d]
6b	503 (1.8)	67 ± 10	5 ± 1
6b(Mo)	532 (3.7)	[d]	[d]
7(Mo)	570 (2.0)	74 ± 11	8 ± 1
8(Mo)	570 (5.3)	[e]	[e]
9(Mo)	495 (3.1)	166 ± 17	17 ± 2
10a	646 (4.7)	316 ± 32	95 ± 10
[10a]$^+$	387 (14.2)	25 ± 4	10 ± 2
10b	563 (4.3)	148 ± 15	13 ± 2
11	538 (6.5)	410 ± 41	8 ± 1
11(Me$^+$I$^-$)	515 (31.1)	[d]	[d]
11(W)	571 (6.3)	306 ± 31	334 ± 4
[11(W)]$^+$	463 (36.1)	[d]	[d]

[a] All compounds are transparent at the fundamental frequency 1064 nm. [b] Measured by HRS at 1064 nm, using *p*-nitroaniline as reference ($\beta = 21.6 \times 10^{-30}$ esu). [c] Data corrected for resonance enhancement at 532 nm using the two-level model with $\beta_o = \beta[1 - (\lambda_{max}/1064)^2][1 - (\lambda_{max}/532)^2]$; damping factors not included. [d] Fluorescence occurs. [e] Response too low to measure.

The first oxidation of **6a(Mo)** undoubtedly occurs at the octamethylferrocene unit, an LMCT band at 589 nm appearing in the spectrum of **[6a(Mo)]$^+$** which is replaced by a stronger absorption at 464 nm on further oxidation to **[6a(Mo)]$^{2+}$**. No weak absorptions in the region 700–1000 nm could be detected, however. The spectra of **[7(Mo)]$^+$** and **[8(Mo)]$^+$** exhibit transitions of modest intensity at *ca.* 570 nm, probably too strong to be d⟶d transitions, but weak transitions consistent with d–d character do evolve between 700 and 760 nm during the second oxidation to **[7(Mo)]$^{2+}$** and **[8(Mo)]$^{2+}$**. The picture is therefore consistent in these complexes, with the ferrocenyl units oxidising first and the molybdenum unit second.

Reduction of the complexes **4(MoCl)**–**9(Mo)** to their mono-anions causes in every case the appearance of a strong band in the red or near-infrared region (770–950 nm), with ε in the range 17,000–22,000 dm^3 mol^{-1} cm^{-1}. We have noted this behaviour before in a variety of simple mononuclear pyridine complexes, [Mo(NO)(Tp^{Me,Me})Cl(pyR)]$^-$,[29] assigning the strong near-IR absorption to an MLCT transition from the 18-electron Mo centre to the π-acceptor pyridine ligand. The presence of a highly conjugated substituent attached to the pyridyl ring will increase the transition dipole moment for the MLCT transition, accounting for the high intensities.

Oxidation of the ferrocenyl group of **6a(W)** and **11(W)** caused the lowest energy bands to shift to higher energy (from 552 to 402 nm, and from 571 to 463 nm, respectively); there being no evidence for the expected ferrocenium-based LMCT transition in the near-IR region. The spectra of **10a** and its mono-oxidised form have been discussed previously and are typical of simple substituted ferrocenes with conjugated substituents.[21]

Nonlinear optical measurements

We have used the hyper-Rayleigh scattering method to measure the first hyperpolarisability, β, of the complexes described in this paper in dichloromethane solution using a laser propagating at 1064 nm. Table 6 shows the measured values of β together with the lowest energy absorption maximum of each complex. The optical nonlinearities of these complexes are resonance-enhanced due to absorption by the CT transition in the region of the second harmonic of the excitation laser (532 nm). We have used the two-level model to calculate the static second-order hyperpolarisability, β_o,[31] the results being included in Table 6. However, given that ferrocenyl derivatives have two charge-transfer transitions, application of the two-level model is problematic to say the least, although it remains in use because of its simplicity and the lack of readily applicable alternatives. The static hyperpolarisability (β_o) values should, therefore, be treated with caution.

From an inspection of the data in Table 7, the following observations can be made. (i) For the series **1** and **2**, there is little difference in the β values for the chloro and bromo complexes, but the iodo complexes have significantly higher β (and β_o) values. (ii) While the measured β value for **1(WCl)** is significantly larger than that for **1(MoCl)**, the rôle of the metal is unclear as the closer proximity of the lowest energy transitions in the former to the second harmonic wavelength of 532 nm would result in a significantly more resonance-enhanced experimental β value. In contrast, the measured β value for **2(MoCl)** is more than three times larger than that in **2(WCl)** but, as stated above, the proximity of electronic transitions to the second harmonic wavelength makes it difficult to comment meaningfully on the effect of metal variation in these complexes. Apparently contradictory changes in β on replacing a first by a second or third row transition metal have been observed by others. Thus the reduction in β caused by replacement of Fe by Ru in metallocene-based dipolar molecules has been attributed to the higher ionisation potential of com-

Table 7 Non-degenerate six-wave mixing results on neutral and reduced compounds

Compound	$\{I_{2\omega}^{6WM}\}^{1/2}$ [a]	μ_{01} [b]/Debye	$\Delta\mu$ [c]/Debye	β^{HRS} [d]/10^{-50} C M^3 V^{-2}	β^{6WM} [e]/10^{-50} C M^3 V^{-2}
2(**MoCl**)	0.22	5.9	10.4	19	29
[**2**(**MoCl**)]$^-$	0.05				7 [f]
3b	0.08	7.6	4.5	32	24
[**3b**]$^-$	0.00				0 [f]
DR1	1.0	7.7 [g]	17 [g]		80 [g]

[a] Six-wave mixing amplitude, normalised on the value for DR1 [4-{*N*-(2-hydroxyethyl)-*N*-ethyl}-amino-4′-nitroazobenzene]. [b] Dipole transition moment; the strongest low-energy absorption at 532 nm was used for this determination. [c] Charge transfer moment in a two-level model description of β^{6WM} (ref. 22), the strongest low-energy absorption at 532 nm was used for this determination. [d] Data from Table 6, conversion factor 1 esu = 0.371 × 10^{-20} C M^3 V^{-2}. [e] From six-wave mixing at 1064 nm; determined using the proportionality relationship $\{I_{2\omega}^{6WM}\}^{1/2} \propto \Delta\mu \times \beta^{6WM}$. [f] β in the reduced compounds is extrapolated from the value for the neutral species using $\{I_{2\omega}^{6WM}\}^{1/2} \propto (\beta^{6WM})^2$. [g] From ref. 41.

parable ruthenocenyl *versus* ferrocenyl moieties, the former group being therefore a less effective donor than the latter.[32] However, replacement of Cr in [Fc–CH=CH-py–{Cr(CO)$_5$}] (py = 4-pyridyl) by Mo and W causes a significant increase in β, but there is little real difference between the results from the second and third row metal complexes.[33] (iii) A comparison of β values of the complexes in series **2** with those of series **1** shows the effect of extending the conjugation of the bridging group; β for complexes in series **2** being around double those of series **1**. The effects of extending the conjugation in the bridge, as demonstrated by series **3**, are more difficult to discern since in both cases the LMCT transitions are very close to 532 nm and there is clearly substantial resonance enhancement of the NLO response. (iv) The data obtained from **4**(**MoCl**), **5**(**Mo**) and **6a**(**Mo**) show that β increases as the extent of methylation of the cyclopentadienyl rings increases. Although the lowest energy transitions are close to 532 nm, the trend is in agreement with the expectation that methylating the ferrocenyl unit makes it a better electron donor. (v) The effect of attaching the metal nitrosyl acceptor to the ferrocenyl–pyridine ligand also has a significant effect on the measured β. As we mentioned above, the acceptor has the effect of moving the relevant MLCT band to lower energy and thereby bringing it closer to 532 nm. So a proportion of the increase in β may be attributed to resonance effects. (vi) The β values of **6a**(**Mo**) and **6a**(**W**) are virtually identical suggesting that the acceptor properties of the two metal fragments are comparable, and (vii) comparison of the β values of **10a** and **10b** shows that the nitro substituent leads to a larger nonlinearity than the formyl substituent which is a poorer acceptor.

Complexes **6b**(**Mo**) and **11**(**Me$^+$I$^-$**) fluoresced when irradiated, and we were unable to extract hyperpolarisability data from them. The HRS response from **8**(**Mo**) was too low to measure.

Effect of chemical oxidation and reduction on hyperpolarisability

The ability to switch the NLO response of a molecule reversibly by controllable perturbations, such as oxidation or reduction, would add significant value to the use of NLO molecules, particularly from the view point of developing molecular photonic devices whose properties can be switched by modifying one of the component parts.[34] There are very few examples of such reversible switching, most of them relying on isomerisation or tautomerisation of the molecule where the conjugated bridge linking the donor to the acceptor undergoes substantial modification.[35]

However, a simple method of controlling the second-order NLO response of a molecule would be a reversible redox change, in which either the donor or the acceptor unit is oxidised or reduced, respectively. We would expect that in either case there would be a substantial loss of the charge-transfer capability of the molecule with a consequent decrease in β.[34] This has been predicted theoretically by the bond length alternation model developed by Meyers *et al.*[36] and described in the two-state approach by Blanchard-Desce and Barzoukas,[37] but there are extremely few examples of this particular effect. Coe *et al.* have described an NLO-active molecule based on an {Ru(NH$_3$)$_5$}$^{2+}$ donor,[38] in which oxidation of the Ru(II) fragment to Ru(III) caused a decrease in the value of β of about one order of magnitude; and similar behaviour was reported by us recently for the reversible oxidation of the ferrocenyl unit of **10a**.[21] Lapinte and co-workers recently described the series of acetylido complexes [Fe(C$_5$Me$_5$)(dppe)C≡CPh]$^{n+}$ (n = 0, 1) and its di- and tri-nuclear analogues 1,3- and 1,4-[{Fe(C$_5$Me$_5$)(dppe)C≡C}$_2$C$_6$H$_4$]$^{n+}$ (n = 0, 1, 2) and 1,3,5-[{Fe(C$_5$Me$_5$)(dppe)C≡C}$_3$C$_6$H$_3$]$^{n+}$ (n = 0–3), where the β values were sensitive to changes in oxidation state although the consequences of reversible oxidation/reduction cycles were not reported.[39]

Oxidation of **6a**(**Mo**) with ferrocenium hexafluorophosphate causes the lowest energy MLCT transition to increase in wavelength from 555 nm to 589 nm, with a consequent decrease by 25% in the value of β. This is a much less dramatic change than that observed on oxidation of **10a** (90% reduction of β),[21] suggesting that while oxidation of **6a**(**Mo**) does attenuate the donor ability of the ferrocenyl moiety, excitation of other parts of the molecule clearly contribute to the charge transfer processes responsible for the hyperpolarisability.

The couple for the formation of [Co(C$_5$H$_5$)$_2$]$^+$ from cobaltocene (−1.34 V *vs.* ferrocene/ferrocenium couple) is sufficient to generate **2**(**MoCl**) from [**2**(**MoCl**)]$^-$ and **3b** from [**3b**]$^-$. This was independently confirmed by observation of characteristic EPR signals from the reduced nitrosyl species, from the differences in the electronic spectra between the neutral and monoanionic species, and by the regeneration of the neutral precursors on oxidation of the reduced species with iodine. Cobaltocene in DMF absorbs very weakly at *ca.* 640 nm (ε 17 dm^3 mol^{-1} cm^{-1}) and at 472 nm (ε 72 dm^3 mol^{-1} cm^{-1}), while the cobaltocenium ion absorbs slightly more strongly at 410 nm (ε 200 dm^3 mol^{-1} cm^{-1}), so it is therefore unlikely that either species would interfere significantly with our attempts to determine the intensity of the second harmonic emitted by either **2**(**MoCl**) or [**2**(**MoCl**)]$^-$. Cobaltocene reduction of **2**(**MoCl**) and **3b** caused a substantial decrease in the SHG signal intensity emitted by these species, namely 76% in the former and 100% in the latter. This was measured by six-wave degenerate mixing (Table 7),[22] and the results show that reduction of the acceptor group in these complexes provides as good a switching mechanism as does oxidation of the donor group in **10a**. Although these oxidations and reductions were carried out chemically, it is also possible in principle to effect them electrochemically,[40] thus opening a route to reversible electro-switching of molecules having second-order NLO properties.

Conclusions

We have described an extensive series of dipolar organometallic complexes in which a ferrocenyl donor is linked to a metal–nitrosyl acceptor *via* a variety of conjugated bridges. Electrochemical and UV/VIS/NIR spectroelectrochemical measurements have been used to characterise the complexes and in

some cases to help determine the order in which different components undergo redox processes.

We have also measured the quadratic hyperpolarisabilities, β, of these, with some interesting results. For the 16-valence electron series **1**–**3**, the value of β is significantly larger in the iodo complexes than in the corresponding chloro and bromo analogues, which is reasonable in the light of the more substantial polarisability of I when compared with Cl and Br. In addition, there appears to be an effect on the NLO response associated with Group 6 metal variation, although the limited data are contradictory. For the species **4(Mo)**–**6a(Mo)**, β increased as the number of methylated cyclopentadienyl rings on the ferrocenyl group increased, *i.e.* as the donor became more electron rich. The acceptor abilities, as implied by the measured value of β, of the fragments $\{Mo(NO)(Tp^{Me,Me})Cl\}$ and $\{W(CO)_5\}$ seem to be comparable.

Finally, oxidation of the ferrocenyl group in **6a(Mo)** and **10a**, and reduction of the molybdenum nitrosyl acceptor in **2(MoCl)** and **3b**, caused the value of β to decrease markedly, suggesting a basis for redox-switchable NLO behaviour. This highlights the utility of redox-switchable groups such as $\{Mo(NO)(Tp^{Me,Me})X\}$ as electron-accepting components in contrast to the simpler organic acceptor groups such as NO_2.

Acknowledgements

We are grateful to the Austrian Foundation for Scientific Research (FWF) for an Erwin Schrödinger Fellowship and the European Community (EC96-0047) (M. M.; R. K.), EPSRC (A. M. M.) and the Leverhulme Foundation (R. L. P.) for postdoctoral fellowships. We also thank the University of Leuven (GOA 2000/03), the Belgian Government (IUAP IV/11) and the Fund for Scientific Research, Flanders (FWO-V G.0407.98 and G.0338.98) for financial support. M. D. W. is the Royal Society of Chemistry Sir Edward Frankland Fellow for 2000/2001.

References

1 *Nonlinear Optical Properties of Organic and Polymeric Materials*, ed. D. J. Williams, American Chemical Society, Washington, DC, 1983, vol. 233; D. J. Williams, *Angew. Chem., Int. Ed. Engl.*, 1984, **23**, 690; *Nonlinear Optical Properties of Organic Molecules and Crystals, I and II*, eds. D. S. Chemla and J. Zyss, Academic Press, Orlando, 1987; *Optical Materials for Non-linear Optics, I and II*, eds. R. A. Hann and D. Bloor, Royal Society of Chemistry, Cambridge, 1989 and 1991; *Materials for Nonlinear Optics, Chemical Perspectives*, eds. S. R. Marder, J. E. Sohn and G. D. Stucky, American Chemical Society, Washington, DC, 1991; *Optical Materials for Non-linear Optics, III*, eds. G. J. Ashwell and D. Bloor, Royal Society of Chemistry, Cambridge, 1993.

2 H. S. Nalway, *Adv. Mater.*, 1993, **5**, 341; N. S. Halway, *Appl. Organomet. Chem.*, 1991, **5**, 349; S. R. Marder, in *Inorganic Materials*, eds. D. W. Bruce and D. O'Hare, Wiley, Chichester, 1992; N. J. Long, *Angew. Chem., Int. Ed. Engl.*, 1995, **34**, 21; D. R. Kanis, M. A. Ratner and T. J. Marks, *Chem. Rev.*, 1994, **94**, 195; H. S. Nalwa, T. Watanabe and S. Miyata, *Adv. Mater.*, 1995, **7**, 754; J. Heck, S. Dabek, T. Meyer-Friedrichsen and H. Wong, *Coord. Chem. Rev.*, 1999, **190–192**, 1217.

3 D. Roberto, R. Ugo, S. Bruni, E. Cariati, F. Cariati, P. Fantucci, I. Invernizzi, S. Quici, I. Ledoux and J. Zyss, *Organometallics*, 2000, **19**, 1775.

4 L. T. Cheng, W. Tam, S. H. Stevenson, G. R. Meredith, G. Rikken and S. R. Marder, *J. Phys. Chem.*, 1991, **95**, 10631; L. T. Cheng, W. Tam, S. R. Marder, A. E. Stiegman, G. Rikken and C. W. Spangler, *J. Phys. Chem.*, 1991, **95**, 10643.

5 B. J. Coe, C. J. Jones, J. A. McCleverty, D. Bloor, P. V. Kolinsky and R. J. Jones, *J. Chem. Soc., Chem. Commun.*, 1989, 1485; L. T. Cheng, W. Tam, G. R. Meredith and S. R. Marder, *Mol. Cryst. Liq. Cryst.*, 1990, **189**, 137; L. T. Cheng, W. Tam, W. F. Eaton and S. R. Marder, *Organometallics*, 1990, **9**, 2856; D. W. Bruce and A. Thornton, *Mol. Cryst. Liq. Cryst.*, 1993, **231**, 253; B. J. Coe, C. J. Jones, J. A. McCleverty, D. Bloor and G. Cross, *J. Organomet. Chem.*, 1994, **464**, 225; D. R. Kanis, P. G. Lacroix, M. A. Ratner and T. J. Marks, *J. Am. Chem. Soc.*, 1994, **116**, 10089; M. J. G. Lesley, A. Woodward, N. J. Taylor, T. B. Marder, I. Cazenove, I. Ledoux, J. Zyss, A. Thornton, D. W. Bruce and A. K. Kakkar, *Chem. Mater.*, 1998, **10**, 1355; J. Mata, S. Uriel, E. Peris, R. Llusar, S. Houbrechts and A. Persoons, *J. Organomet. Chem.*, 1998, **562**, 197; K. N. Jayaprakash, P. C. Ray, I. Matsuoka, M. M. Bhadbhade, V. G. Puranik, P. K. Das, H. Nisdhihara and A. Sarkar, *Organometallics*, 1999, **18**, 3851; G. A. Balavoine, J. C. Daran, G. Iftime, P. G. Lacroix, E. Manoury, J. A. Delaire, I. Maltey-Fanton, K. Nakatani and S. di Bella, *Organometallics*, 1999, **18**, 21; O. Briel, K. Sunkel, I. Krossing, H. Noth, E. Schmalzlin, K. Meerholz, C. Brauchle and W. Beck, *Eur. J. Inorg. Chem.*, 1999, 483; J. Heck, S. Dabek, T. Meyer-Friedrichsen and H. Wong, *Coord. Chem. Rev.*, 1999, **190–192**, 1217; H. Wong, T. Meyer-Friedrichsen, T. Farrell, C. Mecker and J. Heck, *Eur. J. Inorg. Chem.*, 2000, 631; M. Tamm, T. Bannenberg, K. Baum, R. Frölich, T. Steiner, T. Meyer-Friedrichsen and J. Heck, *Eur. J. Inorg. Chem.*, 2000, 1161.

6 J. A. McCleverty, M. D. Ward and C. J. Jones, *Comments Inorg. Chem.*, 2001 in press and references therein.

7 B. J. Coe, J.-D. Foulon, T. A. Hamor, C. J. Jones, J. A. McCleverty, D. Bloor, G. H. Cross and T. L. Axon, *J. Chem. Soc., Dalton Trans.*, 1994, 3427; B. J. Coe, T. A. Hamor, C. J. Jones, J. A. McCleverty, D. Bloor, G. H. Cross and T. L. Axon, *J. Chem. Soc., Dalton Trans.*, 1995, 673.

8 B. J. Coe, S. S. Kurek, N. M. Rowley, J.-D. Foulon, T. A. Harmon, M. E. Harman, M. B. Hursthouse, C. J. Jones, J. A. McCleverty and D. Bloor, *Chemtronics*, 1991, **5**, 23.

9 S. J. Reynolds, C. F. Smith, C. J. Jones and J. A. McCleverty, *Inorg. Synth.*, 1985, **23**, 4; A. S. Drane and J. A. McCleverty, *Polyhedron*, 1983, **2**, 53.

10 A. Wlodarczyk, J. P. Maher, J. A. McCleverty and M. D. Ward, *J. Chem. Soc., Dalton Trans.*, 1997, 3287.

11 B. Bildstein, M. Malaun, H. Kopacka, K. Wurst, M. Mitterböck, K. H. Ongania, G. Opromolla and P. Zanello, *Organometallics*, 1999, **18**, 4325 and references therein.

12 B. J. Coe, C. J. Jones, J. A. McCleverty, D. Bloor, P. V. Kolinsky and R. J. Jones, *Polyhedron*, 1994, **13**, 2107.

13 M. M. Bhadbhade, A. Das, J. C. Jeffery, J. A. McCleverty, J. A. Navas and M. D. Ward, *J. Chem. Soc., Dalton Trans.*, 1995, 2769.

14 B. Bildstein, A. Hradsky, H. Kopacka, R. Malleier and K. H. Ongania, *J. Organomet. Chem.*, 1997, **540**, 127.

15 A. Hradsky, B. Bildstein, N. Schuler, H. Schottenberger, P. Jaitner, K. H. Ongania, K. Wurst and J. P. Launay, *Organometallics*, 1997, **16**, 392.

16 C. Zou and M. S. Wrighton, *J. Am. Chem. Soc.*, 1990, **112**, 7578.

17 D. J. Chadwick and C. Nillbe, *J. Chem. Soc., Perkin Trans. 1*, 1997, 887; B. L. Feringa, R. Hulst, R. Rikers and L. Brandsma, *Synthesis*, 1988, **4**, 316.

18 S.-M. Lee, R. Kowallick, M. Marcaccio, J. A. McCleverty and M. D. Ward, *J. Chem. Soc., Dalton Trans.*, 1998, 3443.

19 M. Stähelin, D. M. Burland and J. E. Rice, *Chem. Phys. Lett.*, 1992, **191**, 245.

20 K. Clays and A. Persoons, *Rev. Sci. Instrum.*, 1992, **63**, 3285; S. Houbrechts, K. Clays, A. Persoons, Z. Pikramenou and J.-M. Lehn, *Chem. Phys. Lett.*, 1996, **258**, 485.

21 M. Malaun, Z. R. Reeves, R. L. Paul, J. C. Jeffery, J. A. McCleverty, M. D. Ward, I. Asselberghs, K. Clays and A. Persoons, *Chem. Commun.*, 2001, 49.

22 B. Paci, C. Schmidt, C. Fiorini, J.-M. Nunzi, C. Arbez-Gindre and C. G. Screttas, *J. Chem. Phys.*, 1999, **111**, 7486 and references therein.

23 G. M. Sheldrick, SADABS, a program for absorption correction with the Siemens SMART area-detector system, University of Göttingen, 1996.

24 G. M. Sheldrick, SHELXS-97 and SHELXL-97, programs for crystal structure solution and refinement, University of Göttingen, 1997.

25 J. A. McCleverty, A. E. Rae, I. Wolochowicz, N. A. Bailey and J. M. A. Smith, *J. Chem. Soc., Dalton Trans.*, 1982, 429; J. A. McCleverty, G. Denti, S. J. Reynolds, A. S. Drane, N. El Murr, A. E. Rae, N. A. Bailey, H. Adams and J. M. A. Smith, *J. Chem. Soc., Dalton Trans.*, 1983, 81.

26 S. L. W. McWhinnie, J. A. Thomas, T. A. Hamor, C. J. Jones, J. A. McCleverty, D. Collison, F. E. Mabbs, C. J. Harding, L. J. Yellowlees and M. G. Hutchings, *Inorg. Chem.*, 1996, **35**, 760.

27 T. N. Briggs, C. J. Jones, H. Colquhoun, N. El Murr, J. A. McCleverty, B. D. Neaves, H. Adams and N. A Bailey, *J. Chem. Soc., Dalton Trans.*, 1985, 1249; N. El Murr, A. Sellami and J. A. McCleverty, *New J. Chem.*, 1988, **12**, 209.

28 J. A. McCleverty and M. D. Ward, *Acc. Chem. Res.*, 1998, **31**, 842.

29 R. Kowallick, A. N. Jones, Z. R. Reeves, J. C. Jeffery, J. A. McCleverty and M. D. Ward, *New J. Chem.*, 1999, **23**, 915.

30 Y. S. Sohn, D. N. Hendrickson and H. B. Gray, *J. Am. Chem. Soc.*, 1970, **92**, 3233; D. Rowe and A. J. McCaffery, *J. Chem. Phys.*, 1973, **59**, 3768; S.-M. Lee, M. Marcaccio, J. A. McCleverty and M. D. Ward, *Chem. Mater.*, 1998, **10**, 3272.
31 J. L. Oudar, *J. Chem. Phys.*, 1977, **67**, 446; J. L. Oudar and D. S. Chemla, *J. Chem. Phys.*, 1977, **66**, 2664; J. Zysss and J. L. Oudar, *Phys. Rev. A*, 1982, **26**, 2016.
32 J. C. Calabrese, P.-T. Cheng, J. C. Green, S. R. Marder and W. Tam, *J. Am. Chem. Soc.*, 1991, **113**, 7227.
33 J. Mata, S. Uriel, E. Pperis, R. Llusar, S. Houbrechts and A. Persoons, *J. Organomet. Chem.*, 1998, **562**, 197.
34 B. J. Coe, *Chem. Eur. J.*, 1999, **5**, 2464.
35 R. Loucif-Saïbi, K. Nakatani, J. A. Delaire, M. Dumont and Z. Sekkat, *Chem. Mater.*, 1993, **5**, 229; S. L. Gilat, S. H. Kawai and J.-M. Lehn, *Chem. Eur. J.*, 1995, **1**, 275; S. Houbrechts, K. Clays, A. Persoons, Z. Pikramenou and J.-M. Lehn, *Chem. Phys. Lett.*, 1996, **258**, 485; K. Nakatani and J. A. Delaire, *Chem. Mater.*, 1997, **9**, 2682; E. Hendrickx, K. Clays, A. Persoons, C. Dehu and J.-L. Brédas, *J. Am. Chem. Soc.*, 1995, **117**, 3547.
36 F. Meyers, S. R. Marder, B. M. Pierce and J.-L. Brédas, *J. Am. Chem. Soc.*, 1994, **116**, 10703.
37 M. Blanchard-Desce and M.Barzoukas, *J. Opt. Soc. Am. B*, 1998, **15**, 302.
38 B. J. Coe, S. Houbrechts, I. Asselberghs and A. Persoons, *Angew. Chem., Int. Ed.*, 1999, **38**, 366.
39 T. Weyland, I. Ledoux, S. Brasselet, J. Zyss and C. Lapinte, *Organometallics*, 2000, **19**, 5235.
40 A. M. McDonagh, J. A. McCleverty, M. D. Ward, I. Asselberghs, K. Clays and A. Persoons, unpublished work.
41 C. Fiorini, F. Charra and J.-M. Nunzi, *J. Opt. Soc. Am. B*, 1998, **15**, 302.